Results of the Simulation of the HTR-Proteus Core 4.2 Using PEBBED-COMBINE: FY-10 Report
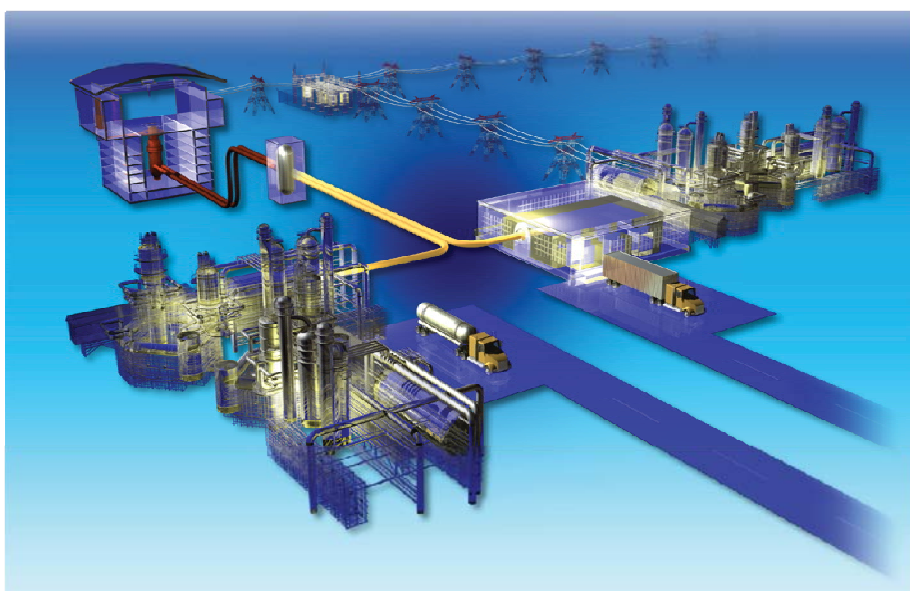
Hans D. Gougar

July 2010

INL
Idaho National
Laboratory

Results of the Simulation of the HTR-Proteus Core 4.2 Using PEBBED-COMBINE: FY-10 Report

Hans D. Gougar

July 2010

Idaho National Laboratory
Next Generation Nuclear Plant Project
Idaho Falls, Idaho 83415

Next Generation Nuclear Plant Project

Results of the Simulation of the HTR-Proteus Core 4.2 Using PEBBED-COMBINE: FY-10 Report

INL/EXT-10-19208

July 2010
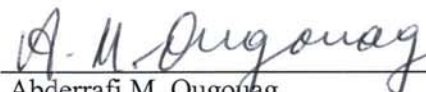
Approved by:

_____
Hans D. Gougar
VHTR TDO Deputy Technical Director

6 July 2010
_____
Date

_____
Abderrafi M. Ougouag
NGNP Methods Physics Lead

06 July 2010
_____
Date

_____
Diane V. Croson
VHTR TDO Deputy Director

7/6/10
_____
Date

ABSTRACT

Deterministic neutronics analysis codes and methods established at Idaho National Laboratory were applied in computing the core multiplication factor of the high temperature reactor-Proteus pebble bed reactor critical facility. These same calculations were performed previously using earlier versions of the codes with less developed methods. The results of that earlier study (reported in INL/EXT-09-16620) indicated that the cross sections generated using COMBINE-7.0 did not yield satisfactory estimates of k_{eff}, concluding that the modeling of control rods was not satisfactory. Over the past year, improvements to the homogenization capability in COMBINE have enabled the explicit modeling of tri-isotropic particles, pebbles, and heterogeneous core zones, including control rod regions, using a new multiscale version of COMBINE in which the one-dimensional discrete ordinate transport code ANISN has been integrated. The new COMBINE is shown to yield benchmark quality results for pebble unit cell models, the first step in preparing few-group diffusion parameters for core simulations. Presented in this report are results of this modeling effort where the full critical core is modeled, but with cross sections generated using the capabilities and physics of the improved COMBINE code. The new PEBBED-COMBINE model enables the exact modeling of the pebbles and control rod region along with better approximation to structures in the reflector. Initial results for the core multiplication factor indicate significant improvement in the Idaho National Laboratory's tools for modeling the neutronic properties of a pebble bed reactor. Errors on the order of 1.6 to 2.5% in k_{eff} are obtained; a significant improvement over the 5 to 6% error generated by previous versions of the code. This is acceptable for a code system and model in the early stages of development, although too high for a production code. Analysis of a simpler core model indicates an over-prediction of the flux in the low end of the thermal spectrum. Reasons for this discrepancy are under investigation. Since new homogenization techniques and assumptions were used in this analysis, further confirmation and validation are required. Further refinement and review of the complex Proteus core model are likely to reduce the errors even further.

CONTENTS

FIGURES

TABLES

ACRONYMS

ACR   automatic control rod

HTR   high temperature reactor

INL   Idaho National Laboratory

LWR   light water reactor

MCNP   Monte Carlo N-Particle

NGNP   Next Generation Nuclear Plant

PBR   pebble bed reactor

TRISO   tri-isotropic

VHTR   very high temperature gas-cooled reactor

WCR   withdrawable control rod

Results of the Simulation of the HTR-Proteus Core 4.2 Using PEBBED-COMBINE: FY-10 Report

1. INTRODUCTION

The Idaho National Laboratory (INL), in support of the Next Generation Nuclear Plant (NGNP) Project, is developing an evaluation model of a candidate pebble bed reactor (PBR) core. This model will be used to investigate critical safety issues associated with the normal and off-normal operation of a pebble bed high temperature reactor (HTR). This model will also be used to compute initial and boundary conditions for integral experiments, such as the Oregon State University High Temperature Test Facility, that will be used to investigate specific scenarios and phenomena.

While Monte Carlo neutronics (N)-Particle (MCNP) codes are extremely accurate for some reactor analyses, they are not well-suited to practical PBR core simulations involving fuel depletion or transient behavior. The corewide power and flux profiles that feed into these simulations change with time. Nodal diffusion codes are comparatively fast and efficient and thus remain the most practical option for safety analysis, sensitivity studies, and core design optimization.

The PEBBED code[1] has been developed at INL for core design and fuel management optimization of PBR cores. PEBBED simultaneously solves the equations of neutron diffusion, depletion, and pebble motion to yield the equilibrium (asymptotic) burnup state of the PBR. PEBBED requires as input the region-wise few-group cross sections required of diffusion and depletion analysis. These cross sections can be supplied directly or computed online using the optional thermal-hydraulic (THERMIX-KONVEK) and spectrum (COMBINE) modules.

PEBBED is a steady state diffusion and burnup code. Transient core behavior resulting from reactivity insertions requires a proper kinetic (time-dependent) diffusion solver. The kinetic complement to PEBBED is the INL code CYNOD. CYNOD models short-term transient behavior such as xenon and rod withdrawal transients, but cannot simulate long-term burnup. PEBBED can provide the initial state of the core (in the form of nuclide densities and cross sections) from which CYNOD then simulates a reactivity transient. Together, these codes can be used to simulate a wide variety of PBR operating scenarios. CYNOD was recently incorporated into the RELAP5 systems analysis code to enable modeling of plantwide phenomena in PBRs.[2]

Neutronic verification of PEBBED has thus far been limited to tests of the standalone diffusion and depletion solvers. The diffusion solver has been verified against solutions to simple core problems for which analytic solutions were computed.[3] This indicates that PEBBED is correctly solving the diffusion equation. This is not a validation, however, because diffusion theory may not be valid for some reactors nor does it infer any information about the assumptions and approximations made in constructing a PEBBED model of an actual reactor. The depletion solver was verified by comparing burnup and specific nuclide concentrations under various conditions against the pebble bed modular reactor code VSOP99.[4] In all of these cases, cross sections were supplied to PEBBED for subsequent diffusion or depletion analysis.

Validation of a core model requires comparisons to actual physical systems. Low power critical reactors have been designed and operated for neutronic validation. The PROTEUS facility in Switzerland operated from 1992 to 1996 in support of HTR research programs.[5] The reconfigurable core was used to validate both prismatic and PBR physics codes. Core 4 of the campaign was a randomly loaded pebble bed core, and was thus used in this study to validate the INL suite of deterministic PBR physics tools. This report summarizes the results of a recent modeling effort intended to test and validate the code system with an improved cross section capability.

This study is a follow-on to a similar one completed in 2009 and reported in INL/EXT-09-16620.[6] This report is intended to provide a measure of the improvement in the ability of INL and the NGNP Project to model the neutronics of complex PBRs and to identify issues for which further methods development efforts may be needed.

2.   PROTEUS CRITICAL FACILITY

2.1   History and Basic Core Configuration

Proteus is a zero-power research reactor operated by the Paul Scherrer Institute in Switzerland. The basic geometry is that of a cylindrical graphite annulus with a central cylindrical cavity (see Figure 1). The graphite annulus remains basically the same for all experimental programs, but the contents of the central cavity are changed according to the type of reactor being investigated. Through most of its service history, Proteus has represented light water reactors (LWRs), but from 1992 to 1996, Proteus was configured as a PBR critical facility and consequently designated as HTR-Proteus. During this period, 13 critical configurations were assembled and various reactor physics experiments were conducted.
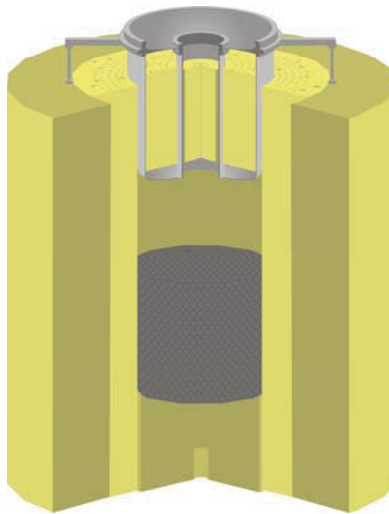
Figure 1. Cutaway view of Proteus with core, inner, and outer reflectors.

These experiments included measurements of criticality, differential and integral control rod and safety rod worths, kinetics, reaction rates, water ingress effects, and small sample reactivity effects.

HTR-Proteus was constructed, and the experimental program was conducted to provide experimental benchmark data for assessment of reactor physics computer codes. Considerable effort was devoted to benchmark calculations as a part of the HTR-Proteus program. References 7 and 8 provide detailed data for use in constructing models for codes to be assessed. Reference 5 is a comprehensive summary of HTR-Proteus experiments and the associated benchmark program. This document draws freely from these references. Section 2 provides a simple description of the geometry.

2.2   Physical Geometry and Structure

The fuel elements in any PBR are spherical "pebbles" roughly the size of billiard balls, composed of a graphite matrix in which thousands of tiny (approximately 1 mm diameter) coated fuel particles are embedded. In an operating PBR, the pebbles are dropped into the core from one or more drop points above the core and removed at the bottom, so that the core slowly flows downward, and the pebbles are normally circulated through the core several times (typically about 10) before they are discarded after reaching their burnup limit. During their passage through the core cavity, they acquire a random and continually changing arrangement. It is possible to define a randomly loaded pebble bed for modeling

purposes, but such a model only represents one of an infinite number of possible arrangements. The probability of a randomly loaded model accurately representing an actual specific randomly loaded experiment is essentially zero.

Thirteen critical configurations were assembled in the HTR-Proteus experimental program. These configurations differed in the arrangement of their cores. In three of the experimental configurations (Cores 4.1, 4.2, and 4.3) the pebbles were randomly loaded into the central cavity. In the remaining 10 configurations, the pebbles were arranged manually into lattices. The experimenters used the term "deterministic" to denote these regular cores. These lattices were either hexagonal close-packed or hexagonal point-on-point configurations. The former arrangement is like oranges in a crate as shown in Figure 2. In the latter configuration, the pebbles are in successive layers that form columns without any relative lateral displacement. These deterministic arrangements are considered much more useful for benchmarking reactor physics computer codes. In fact, they have been the focus of benchmarking activities in the NGNP Methods program.[9] The randomly loaded cores, however, better reflect the designs proposed for commercial reactors, including the PBMR400.[10]
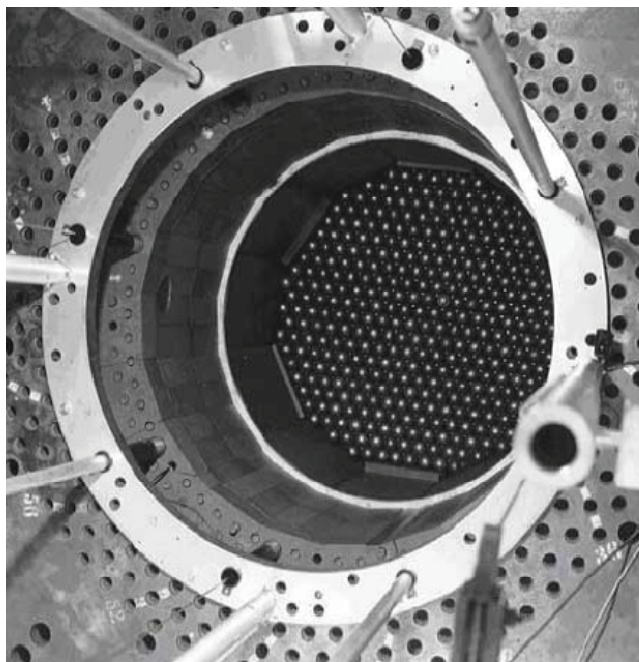
Figure 2. Top view of a PROTEUS deterministic core.

HTR-Proteus Core 4 was loaded by dropping pebbles into to the core cavity from a loading tube suspended above the core. This core has not yet been modeled with MCNP, given the difficulty in defining the locations of randomly located pebbles in the MCNP model, and comparisons with PEBBED results are therefore not obtainable. The homogenization process used in building PEBBED models is not affected by the random nature of fuel loading; indeed the computation of the Dancoff factors used in the generation of cross sections with PEBDAN explicitly takes this randomness into account.

A schematic side view of the HTR-Proteus facility is shown in Figure 3.
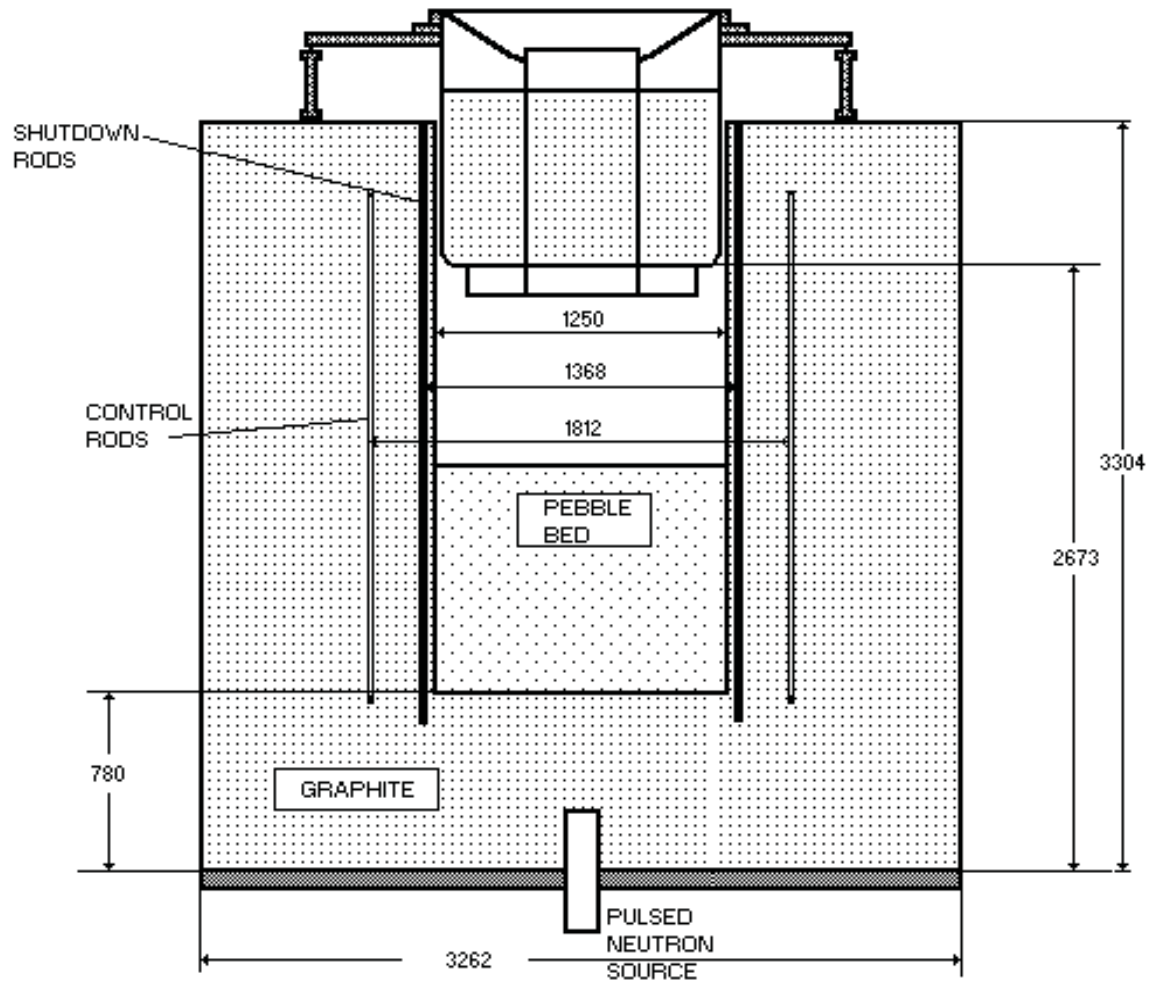
Figure 3. Schematic side view of the HTR-Proteus facility (dimensions in mm), taken from Reference 8.

The reflector consists of three basic regions, the lower axial reflector, the radial (or side) reflector, and the upper axial reflector. The radial reflector extends from the core cavity radial boundary to the outer radial boundary of the reflector and from the base of the reflector upwards to a height of 3,304 mm. The lower axial reflector is the reflector region below the core cavity, and the upper axial reflector is the region above the core cavity. The upper axial reflector is suspended above the core cavity and extends above the top of the radial reflector as shown above. No information has been obtained regarding the number or azimuthal extent of the support structures that suspend the upper axial reflector.

The upper axial reflector is a complex structure containing graphite, aluminum, and steel. It includes inner and outer aluminum tanks, an aluminum safety ring to prevent the upper axial reflector from accidently falling onto the pebble bed, and a steel lid, support plate, and flanges.

The lower axial reflector has a boring in the bottom for placement of the pulsed neutron source, which was not modeled in this study. It also contains 160 symmetrically located borings 27.43 mm in diameter, of which at least 127 (the exact number depends on the core configuration) are filled with graphite rods 26.5 mm in diameter for the entire height of the lower axial reflector. The remainder of the borings serve as coolant channels, which remain open to the core cavity. These coolant channels, when not filled with graphite, are located at radii of 300, 410, and 515 mm and angles at 16.875, 50.625, 84.375, 118.125, 140.625, 174.375, 208.125, 241.875, 275.625, 309.375, and 343.125 degrees clockwise

5

from a reference angle (the +x-axis shown in Figure 4). The upper axial reflector contains coolant channels located in the same places as the coolant channels in the lower axial reflector, plus an additional one on the core centerline. In the upper axial reflector, these 34 channels are always open.

A graphite structure called the thermal column is 1,200 mm high by 1,200 mm wide on one side of the radial reflector, as shown in Figure 4. Its radial depth is about 500 mm. It extends from a level of 984 mm above the bottom of the radial reflector upwards to a level of 1,120 mm below the top of the radial reflector.
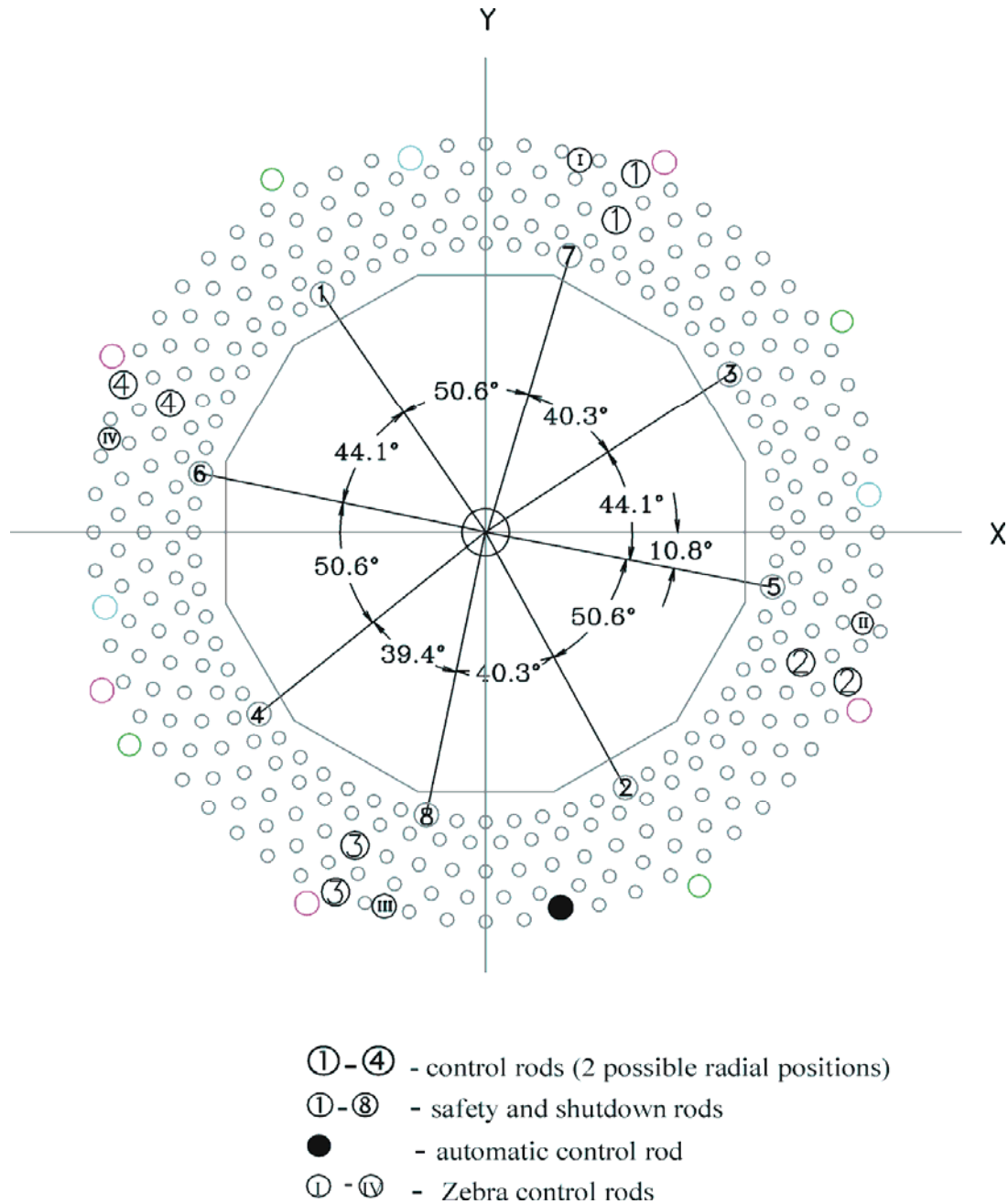
Figure 4. Cross section through core region showing borings in radial reflector and locations of safety/shutdown rods and control rods, taken from Reference 8.

Finally, the entire reactor system is surrounded by concrete shielding. None of the available references provided any information regarding the thickness of the concrete. For this study, a thickness of 1 meter was assumed for a shield composed of Portland cement.

Figure 4 also shows a horizontal cross section through the core region of a generic experimental configuration. This figure shows numerous borings in the reflector near the core, some of which are occupied by control elements of various kinds.

The borings in the radial reflector are designated as C-Driver locations. They are arranged in five rings. The first, third, and fifth rings are aligned radially, while the second and fourth rings are shifted azimuthally one-half of the angular spacing between borings in a ring. There are 320 of these borings, which are 27.43 mm in diameter. More than 300 of them were filled with graphite rods 26.5 mm in diameter, but some locations were used for control rods and safety/shutdown rods.

The radial outer boundary of the radial reflector is shaped as an irregular 22-sided polygon 3,262 mm across, as shown in Figure 5. The radial inner boundary of the radial reflector is a similar irregular 22-sided polygon 1,250 mm across the flats. Note that one of the inner flats, at 62 mm wide, is smaller than the others at 185.5 mm.

For the hexagonal close-packed cores, additional spacers were placed in alternate layers to fill the gaps created by the horizontal displacement of these layers relative to the adjacent layers. These spacers were not used in the stochastic cores, but wedges were placed around the bottom of the core cavity to simulate a conical discharge region.

The pebbles were loaded via drop tubes while the top reflector was removed. The fuel pebbles each contained slightly fewer than 5,000 tri-isotropic (TRISO) particles with a heavy metal loading of uranium enriched to 20% U-235. Pure graphite (moderator) pebbles were also loaded in specified proportion to the fuel pebbles. For Core 4.2, the fuel-to-moderator pebble ratio was 1:1. Core 4.1 was omitted because the nature of the pebble loading mechanism. A single moveable tube provided the pathway for both fuel and moderator pebbles. There were, however, doubts about the randomness of the fuel and moderator pebble distribution. For Core 4.2, the single tube was replaced by a double tube through which moderator and fuel pebbles could be dropped simultaneously.

Reactivity is controlled using a fixed but withdrawable control rod (WCR) and a moveable automatic control rod (ACR). The WCR consists of two concentric stainless-steel tubes inserted through most of the core. The ACR consists of a copper bar with a rectangular cross section suspended in an aluminum tube. The bar is tapered in the axial dimension so that it resembles a long thin wedge pointing downward into the core. This rod is partially inserted into the core with its position maintained by reactivity control logic.

The two rods are not located along the same radial-axial plane, so the core has no azimuthal symmetry with which to build an accurate RZ core model. For simplicity, however, PEBBED RZ models were constructed by homogenizing the rod materials around in a gray curtain in such a manner so as to preserve the reaction rates occurring in the discrete absorber materials. This process will be discussed in Section 3.3. Full 3-D models with two discrete rod channels have also been constructed, however, execution of these models is hampered temporarily by file format and conversion errors encountered while running the new COMBINE on the high performance computing platform. These problems are being resolved. A full 3-D reactor model demands considerable internal memory by PEBBED's combination diffusion, spectrum, and thermal fluid modules.
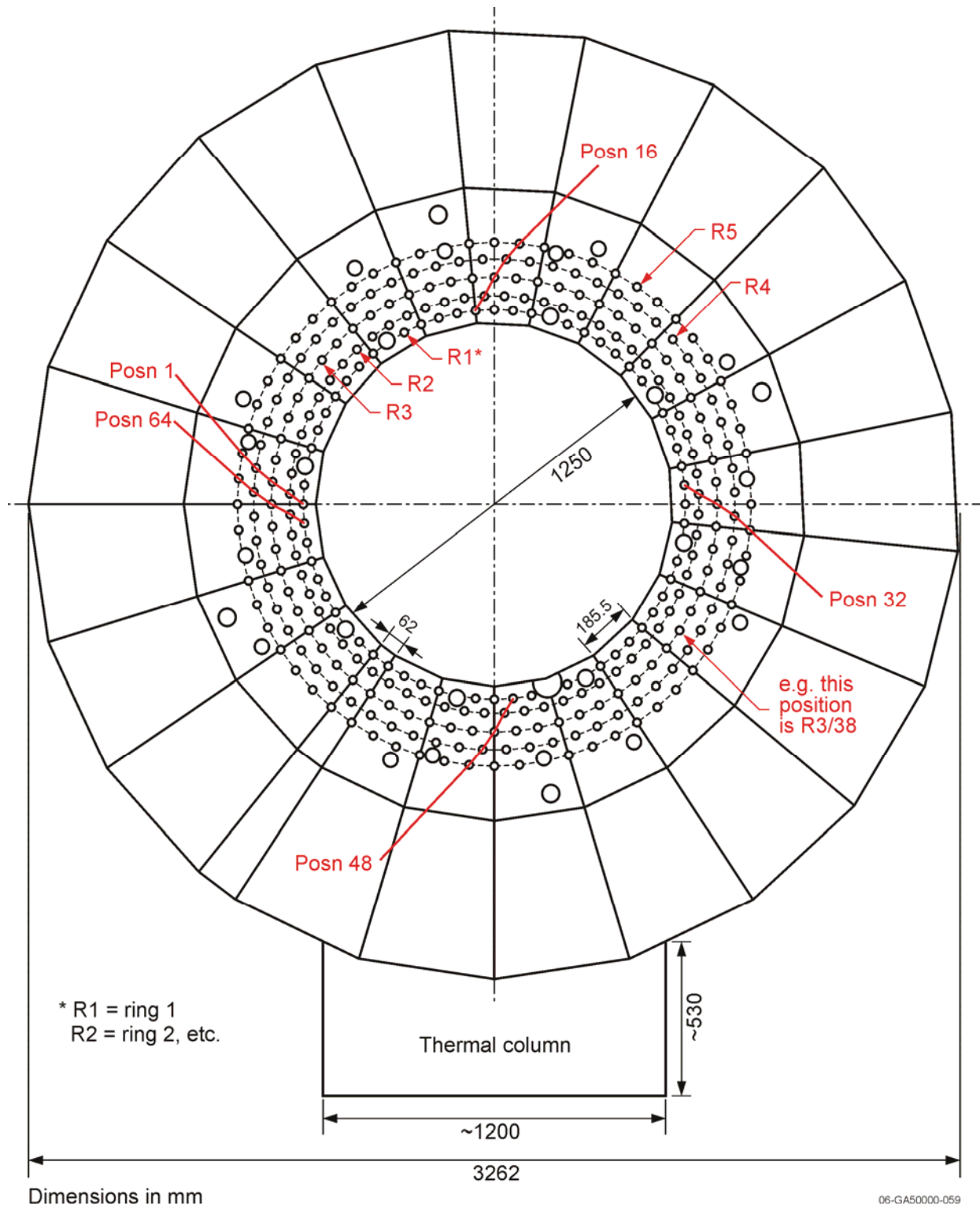
Figure 5. Details of radial reflector and cavity, taken from Reference 7.

3. PROTEUS EVALUATION MODEL

3.1 Acceptance Criteria for this Critical Evaluation

Critical evaluations are usually performed using high fidelity Monte Carlo or deterministic transport codes. It is practical to use these tools for critical core evaluations because the reactor is held at a constant, almost uniform temperature through the structure and at a constant power. Thermal fluid and transient capabilities are thus not required of the code. Monte Carlo models of critical facilities are usually quite detailed; models are in 3-D, individual coolant holes are modeled, the exact shape of absorbers are preserved, and so on. Furthermore, Monte Carlo codes like MCNP and a small number of experimental deterministic codes do not make the discrete energy (multigroup) assumption common to core simulators, but can exploit the continuous or highly resolved range of values in nuclear data libraries. Therefore, these models can have a fidelity that is limited only by the geometric detail retained by the modeler and the accuracy and completeness of the material specification and nuclear data libraries. It is not uncommon to obtain errors in the core multiplication factor (eigenvalue or k_{eff}) of less than 1%. Errors between 0.2 and 0.7% were obtained by the INL for MCNP evaluations of the other, regularly loaded, Proteus cores.[9] Such efforts reveal biases and can provide an indication of the sensitivity of the core multiplication factor to some material parameters. In recently completed evaluations of the Japanese High Temperature Test Reactor, a computational bias of 2 to 3% was observed in all of the results of the participants.[11,12] Much of this is postulated to be the result of an incorrect specification of the boron content in the graphite blocks; a parameter to which the eigenvalue is quite sensitive. A similar result was obtained using the deterministic codes DRAGON and HEXPEDITE[13] as part of a demonstration of the modeling tools being developed for NGNP by INL.

As PEBBED-COMBINE was written for computationally demanding fuel management and core design calculations, it relies more heavily upon approximations in order to realize short runtimes. Using 1-D transport rather than 2-D or 3-D to generate cross sections and multigroup diffusion rather than continuous energy transport for the core calculation necessarily compromises accuracy. Combined with simplifying assumptions for some core structural features, the uncertainty in neutronic results is expected to be higher than what is achievable with the high fidelity tools. For HTR core analyses, an uncertainty of $\pm 1.5\%$ in k_{eff} is considered acceptable.[14] For this preliminary test of a new code and modeling approach, an error of $\pm 2.5\%$ is targeted. It is expected that further refinements of the code using modern physics methods and procedures will eventually reduce the uncertainty to a more acceptable level of $\pm 1.0\%$

3.2 Computational Tools and Sequence

The deterministic transport tools COMBINE-7.1 and PEBBED were deployed to produce axial, radial, and full core flux profiles and the core multiplication factor (or eigenvalue as denoted by k_{eff}). The embedded transport solver ANISN was used in place of the SCAMP code used in the preceding study.[6] Because almost all PBR power plants feature randomly loaded cores and because PEBBED, COMBINE, and THERMIX-KONVEK currently comprise the foundation of the INL's PBR core design and fuel management capability, it was proposed to validate this suite of deterministic codes using Proteus Core 4. The core multiplication factor (k_{eff}) is a direct measure of the ability of these tools to reproduce and predict neutronics reaction rates and flux distributions. Flux profiles could also be generated, but there is limited data (measurements) against which these profiles can be compared. The principal measure of success of the codes and methods in this study is therefore k_{eff}. The other computed data can be used for speculation about sources of error.

Deterministic models like these employ a homogenization step in which the model is discretized into regions (nodes) over which a neutron balance is computed. The geometric details within each node are used to generate equivalent diffusion theory parameters for the homogenized regions. The diffusion

equation is then solved over the ensemble of homogenized (internally uniform) nodes. The process is the same whether the fuel is randomly distributed within the node or arranged in an ordered (crystalline) lattice. The generation of homogenized diffusion parameters for core analysis must account for numerous complex phenomena such as resolved and unresolved resonance interactions, shadowing by neighboring fuel lumps, and self-shielding within those lumps.

INL has been engaged in the development of deterministic tools for PBR analysis. The PEBBED code is the only tool under development within the United States that can simulate neutron transport and burnup in recirculating PBR cores. The COMBINE[15] spectrum generation code has been modified to compute few-group transport and diffusion coefficients for PBR nodal calculations. COMBINE has been incorporated into PEBBED as a subroutine for inline cross section generation. The heterogeneity of different core and reflector structures has a significant effect upon the local neutron spectrum which must be captured in the cross section generation process through approximate methods or explicit and detailed neutron transport calculations. One of the effects upon the resonance absorption is the 'shadowing' of a fuel lump (kernels or pebbles) by its neighbors. An accepted way of treating this phenomenon is through a modification to the Wigner rational approximation using so-called Dancoff factors. PEBDAN[16] generates Dancoff factors for randomly dispersed pebble bed fuel, and PEBBED accepts these factors in the input. The other major effect of heterogeneity is thermal self-shielding in which low-energy neutrons are absorbed in the outer layers of an absorber and the thermal reaction rate in the interior is effectively reduced. The previous version of COMBINE used a rough approximation[15] for the thermal self-shielding that is inadequate for HTR fuel. Thermal self-shielding is now captured explicitly and automatically using the ANISN discrete ordinates module in COMBINE and it does so for both the particle and pebble levels of heterogeneity. In the previous study, the SCAMP 1-D discrete ordinates code was used to generate cross sections in all noncore nodes. A 1-D SCAMP cylindrical model of each axial plane was constructed and driven by 99-group cross sections from COMBINE pebble unit cell calculations. From the transport solution, cross sections for each side reflector node were then coalesced into the few-group structure of PEBBED. The ANISN module of COMBINE now performs this function but in 167 groups.

For generating the core neutron spectrum, COMBINE-7 solves the 0-D B-1 or B-3 approximations to the neutron transport equation in a unit cell (node). COMBINE-7 uses ENDF/B-VII data libraries processed with NJOY9932 to solve for the flux over the entire energy range (2E7 to 1E-5 eV). This avoids the limitation of many legacy unit cell spectrum codes that have separate thermal and fast spectrum modules and are unable to treat upscattering and low-energy resonances simultaneously. COMBINE-7 uses the Bondarenko method for treatment of the unresolved resonance region and either the Bondarenko or Nordheim numerical method for resolved resonances. For HTR fuel, the difference between the results of these two treatments was found to be negligible so the much faster Bondarenko treatment was used throughout.

The new version of COMBINE features a multiscale homogenization capability for generating cross sections for the pebbles. The slowing down calculation is performed for the kernel and this source drives a 1-D spherical transport model of the TRISO particle and surrounding matrix graphite. The particle-averaged cross sections are then inserted into the fueled interior region of a 1-D spherical model of a pebble. 167-group cross sections again are coalesced using the transport solution to yield homogenized cross sections for a fuel region unit cell. Finally, the homogenized pebble cross sections are inserted into a 1-D cylindrical model of the reactor core, which includes different core, reflector, gas gap, and vessel regions. An ANISN model of this wedge executed (again in 167 groups) to generate leakage-corrected spectra and cross sections for each core and reflector node. Axial and azimuthal leakage is captured approximately with few-group transverse leakage terms in the transport equation. This 3-stage homogenization process retains the maximum fidelity achievable within the limits of the B-1 and discrete ordinates transport approximations (see Figure 6). Because transverse leakage must be computed form the core diffusion solution, the spectrum and diffusion modules must be solved iteratively to yield a converged flux solution.
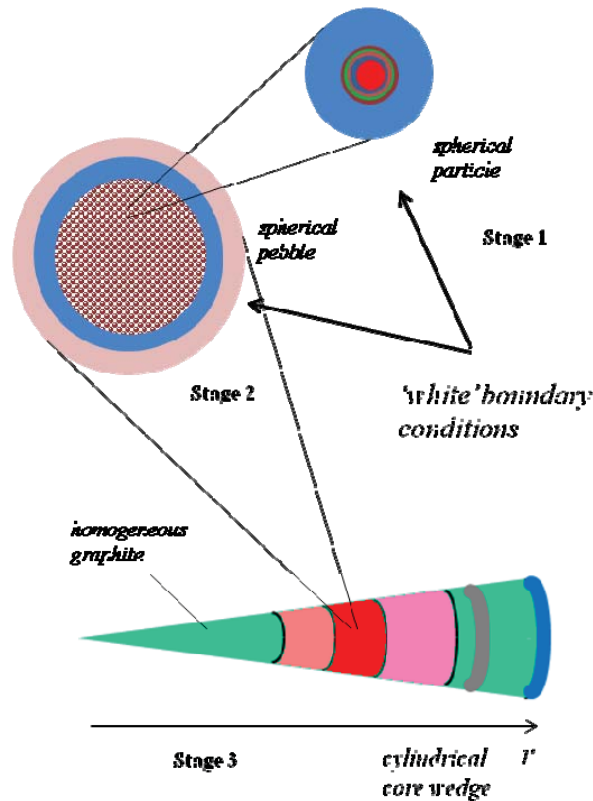
Figure 6. 3-Stage Model for PBR Core Homogenization.

This approach to cell homogenization is known to not preserve the interpebble leakage rates in the resulting diffusion coefficients. The correction developed by Lieberoth and Stojadinovic[17] is therefore applied to adjust these values to account for interpebble streaming. Also, the streaming of neutrons across void regions such as the gas plenum above the pebble bed is not treated accurately with cell codes such as COMBINE. Gerwin and Scherer[18] developed an analytical treatment that yields diffusion coefficients for the gas plenum between the top of the core and the top reflector. These values are supplied in the PEBBED input and replace those generated using COMBINE.

Rather than interpolate cross sections from tables computed prior to the core simulation, PEBBED integrates the diffusion and spectrum generation calculations into one iterative sequence. This requires that the detailed particle, pebble, and reflector morphology (layer dimensions and material compositions) be fully specified in the PEBBED input. PEBBED then constructs and executes detailed COMBINE input files from this data. A pebble-mixing subroutine computes the node-averaged pebble composition if pebbles of different types and burnups are present with a node. The PEBBED input specification was extensively modified to support this capability.

This capability is also used to generate cross sections for the control rods and other reflector structures. The rods usually consist of an absorber material embedded inside one or more metal tubes and lowered into holes drilled into the side reflector blocks (see Figure 7). A 1-D cylindrical model can capture the shape of these structures if axial leakage is ignored and a cylindrical shape is assumed for the surrounding graphite block. Likewise, metal support plates and blocks above and below the core can be modeled with ANISN in 1-D Cartesian symmetry to capture transport effects. Again, the user supplies the detailed shape and composition of the control rod or reflector node in the PEBBED input. Homogeneous (0-D) compositions can be defined for regions without absorbers or structure as simple mixtures of materials.
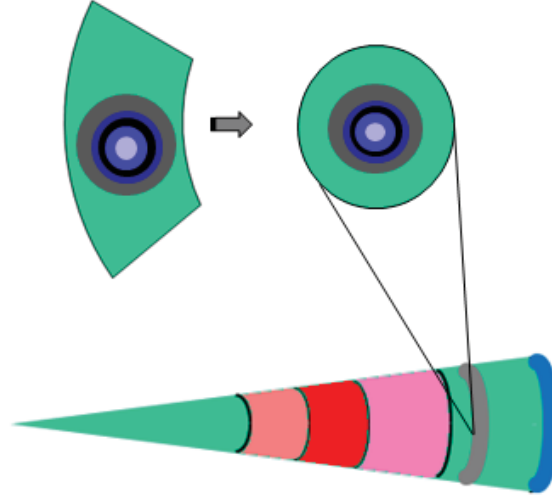
Figure 7. Control rod nodes in a PEBBED cylindrical wedge subregion of the core.

3.2.1   Modeling Sequence

1. A PEBBED core model is constructed using the benchmark specification. The core model is divided into nodes, and a set of cross sections will be computed using COMBINE (see Figure 8) for each node. Dimensions of the major core structures are shown in Appendix A, Figure A-1. Compositions were defined and assigned to each node (see Table A-1). Masses and volumes of structures within each node were converted to number densities. PEBDAN was run to generate spatially varying packing fraction and Dancoff factors. Particle and pebble structural and material details were computed from the benchmark specification and used to define the core composition. Number densities for the pebble bed zone are shown in Table A-2.

2. Control rod and reflector geometry and materials were similarly specified and defined in PEBBED as 0-D or 1-D compositions (see Tables A-3 through A-5). The core is divided into four azimuthal sectors; a small sector for the WCR, a small sector for the ACR, and two large sectors for the solid graphite reflector between the control rods (NCR×2). In effect, four RZ models were constructed and combined to form one 3-D model.

    The WCR is a concentric pair of stainless-steel tubes so their geometry can be modeled exactly with the cylindrical solver of ANISN. The ACR is a rectangular copper bar that tapers from a 3.91 cm length at the top down to a point over its 230.0 cm height.

3. When PEBBED is invoked, it reads the composition specifications and constructs and executes all of the necessary COMBINE input files. The microscopic cross sections for each spectral zone are generated by COMBINE and stored in multidimensional arrays. PEBBED then constructs the macroscopic diffusion parameters from these arrays and the zone-averaged number densities. The diffusion equation is then solved over the model mesh. Once converged, the internodal currents are used to compute the buckling terms that COMBINE uses to adjust the 0-D or 1-D cell calculations for transverse or total cell leakage. This leakage does affect the spectrum nor the microscopic cross sections generated by COMBINE so the sequence must be repeated until the total core k_{eff} and the individual zone multiplication factors all converge.

    In this manner, the R-Z model of the ACR was first executed. Although not an accurate reflection of the full core, this model yielded microscopic cross sections for the materials in the ACR (copper and aluminum).
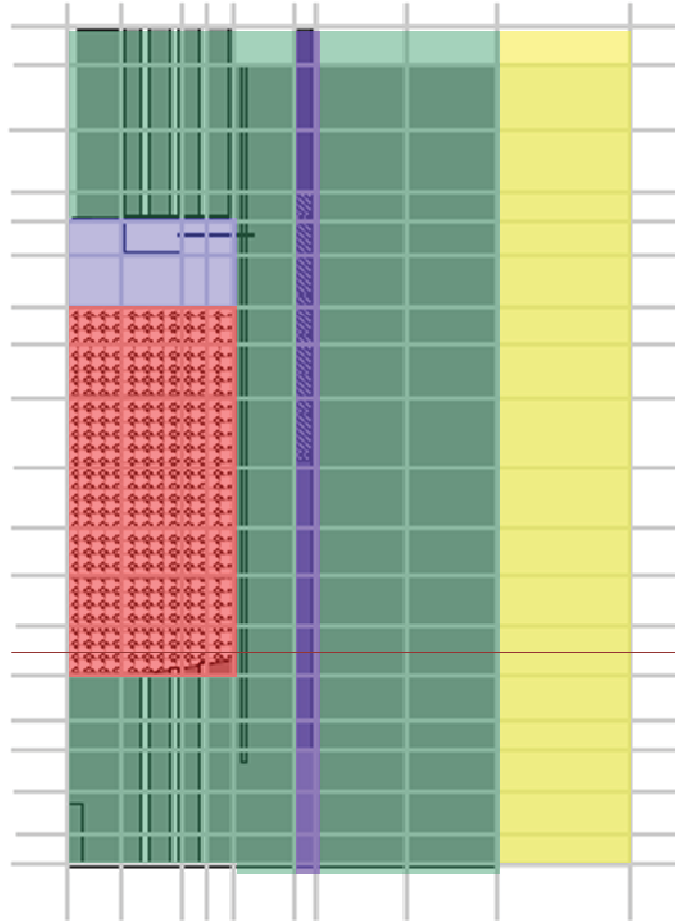
Figure 8. RZ model of the Proteus facility showing major
core regions and node boundaries.

4. The WCR model was then executed but with the densities average over the entire azimuthal dimension (360 degrees). Because the precise dimensions of the WCR are specified and used to build the COMBINE model, the resulting microscopic cross sections generated for the control rod zone materials (stainless steel and graphite) reflect the correct rod geometry. The data from the ACR model in Step 3 were manually added to the cross section files of these zones. The azimuthally averaged number densities of the ACR materials were added to the control rod node specification in the PEBBED model. The combination of smeared number densities and microscopic cross sections generated using the explicit geometry model will, in theory, yield equivalent reaction rates in the 3-D core.

Steps 5 and 6 can be omitted in modeling the core in 3-D. All four azimuthal compositions are included explicitly in the PEBBED model.

5. Diffusion coefficients for the void space above the core were hand computed for the void region using the Gerwin and Scherer method. The diffusion coefficients of the pebble bed were adjusted in COMBINE using the Lieberoth and Stojadinovich method. The diffusion coefficients for the remaining nodes were computed by COMBINE using the traditional homogenization algorithm. Core eigenvalue results from the 2-D (RZ) and 3-D models were compared to the benchmark experimental value.

6. A duplicate analysis was performed, but the core packing fraction was assumed to be uniform throughout rather than varying in the radial direction as estimated by the PEBDAN code.

3.3   Computational Models, Assumptions, and Approximations

The assumptions and approximations used in this analysis are described in this section. All contribute to the uncertainty in the final result, although computing the full sensitivity to each is beyond the scope of this study.

3.3.1   Energy Discretization

Most core simulations of HTR transients and fuel cycles use the multigroup approximation; i.e., the energy spectrum of neutrons is discretized into a small number of contiguous energy groups. Within each group the neutron balance equation is solved as if the neutrons all have the same energy with the groups coupled by group-to-group scattering cross sections. The groups should be chosen to capture the major types of neutron interactions (birth from fission, unresolved scattering, resolved resonance scattering, thermal scattering, etc.). A large number of groups is required for generating cross sections and the COMBINE code performs all slowing down and resonance processing in 167 groups spanning the range of 0 electron volts (eV) to 20 MeV.[15] Core calculations are performed in a smaller set of groups condensed from this set. In the PEBBED analyses, two different coarse group structures were used as shown in Table 1; one with four groups and one with 16 groups. No optimization of the group structure was performed for this study; the spectrum was simply divided into approximately equal lethargy intervals. The NGNP Project supports research into group structure optimization techniques.

Table 1. Coarse group structures used in the PEBBED analyses.

Group Number	Maximum Energy (eV)	
	Structure 1	Structure 2
16 (4)	2.0E07	2.0E07
15	3.68E06	
14 (3)	8.21E+05	8.65E+07
13	1.83E+05	
12	3.18E+04	
11	7,102	
10	1,234	
9	354	
8	78.9	
7 (2)	13.7	29.0
6	2.38	
5 (1)	1.9	1.9
4	1.5	
3	.89	
2	.42	
1	.12	

3.3.2   Spatial Discretization of the Spectral Mesh (Nodalization)

Because the major regions of the core consist of different materials and neighbors, the cross sections for these materials will vary in space. One can, however, expect that the loss in fidelity is small by assuming cross sections are roughly constant within smaller regions of the model. These regions are the nodes and the boundaries are determined by major material discontinuities (e.g., core-reflector interface) or by engineering judgment. Unlike LWRs with well-defined assemblies, zone boundaries within the pebble bed itself can be arbitrarily chosen. Recent research at Penn State University, with support from

the NGNP Project, has resulted in a rigorous method for optimizing the location of node boundaries to yield the best agreement with an analytical solution. This method is still being implemented in the code package and thus was not applied in this study.

3.3.3 Spatial Discretization of the Diffusion Mesh

In the finite difference approximation to the diffusion equation, an algebraic difference equation is used to approximate the 2nd order differential equation that represents the neutron balance within a control volume. Truncation error is inherent in this approach but can be minimized by reducing the size of the individual control volumes (mesh refinement). The spatial mesh in this study was refined until there was no appreciable change in bulk core parameters.

3.3.4 Spatial Discretization of the Transport Mesh

The models of the particle, pebble, and radial core were also discretized for the ANISN transport solution. A mesh spacing of 0.5 to 1 mean free paths was used in each layer, as per the ANISN user manual. A angular discretization of order 12 was used for the scattering angle.

3.3.5 Homogenization of the Fuel Zones (Pebble Bed)

Because the ANISN discrete ordinates solver in COMBINE is limited to one dimension, every node within the model that possesses some geometric structure must be modeled as an infinite slab, infinite cylinder, or sphere. The pebble bed in the Proteus reactor consisted of a 50/50 mixture of fueled and pure graphite pebbles surrounded by coolant. A unit cell was constructed with a 5 cm (diameter) fuel region consisting of TRISO particles embedded in a graphite matrix (as specified for a single Proteus fuel pebble). This fuel zone was surrounded by the usual 0.5 cm graphite shell. An additional layer of graphite was then added to this shell with a volume and density corresponding to that of the graphite-only pebbles. The volume of the surrounding coolant equals the sum of the coolant volumes surrounding a single fuel and a single graphite pebble. This spherical unit cell retains the masses and volumes of the materials found in each fuel/moderator pebble pair. It also possesses the correct TRISO particle geometry and packing structure so that the proper shadowing and thermal self-shielding attributes are preserved. Figure 9 illustrates the pebble arrangement in the core region and the corresponding unit cell modeled in COMBINE. The dotted line in the unit cell pebble (right) indicates the nominal fuel pebble boundary.
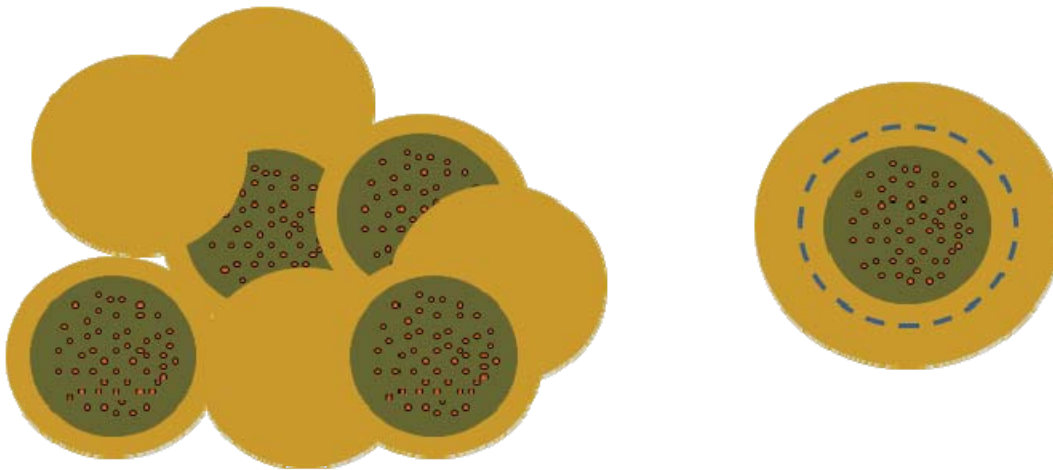
Figure 9. 1-D Spherical Unit Cell for the Fuel Region.

As part of the Proteus benchmark specification, a number of unit cell computational benchmarks were defined to test the users' ability to model the fuel. These unit cell benchmarks differed in the arrangement of pebbles (random or ordered) and the ratio of fuel to moderator pebbles. The randomly ordered cases were modeled in the manner described in the previous paragraph. Unfortunately, no results of this particular case are available in the open literature. Further inquiries are underway to find or generate unpublished results so that the COMBINE results can be compared to other methods and codes. It can be noted, however, that preliminary COMBINE unit cell results for a single pebble (no moderator pebbles) compare favorably to MCNP and other published results (see Table 2).[19] This indicates that the COMBINE 1-D unit cell calculations are as accurate as other computational approaches and codes.

Table 2. Multiplication factor results for three unit cell pebble models.

Model	UO_2	PuO_2	ThO_2/UO_2
MCNP*	1.5234	1.4584	1.4710
NEA Monte Carlo mean	1.5115	1.4611	1.4631
NEA Deterministic Mean	1.5127	1.4692	1.4629
COMBINE	1.5168	1.4576	1.4723

* Unpublished result from INL models of a pebble with 15,000 randomly placed TRISO particles.

3.3.6   Homogenization of the Fuel Zone/Discharge Cone Wedge Zones

Recirculating PBRs contain a sloped lower reflector to facilitate the movement of pebbles into the discharge chutes. This conical shape of the pebble bed lower boundary (conus) can be modeled in many codes that feature explicit geometry capability, but other codes (like the current version of PEBBED) assume a flat bottom to the core. In Proteus Core 4, graphite wedges were placed on the top of the lower reflector to simulate the geometry and neutronics of the conical lower reflector, shown as the shaded areas in Figure 10.
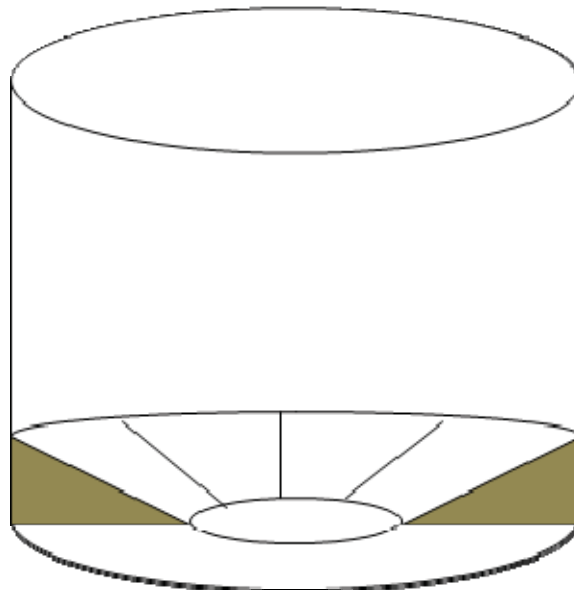
Figure 10. Outline of pebble bed core with wedge blocks.

The orthogonal (R-θ-Z) mesh employed by PEBBED requires that these wedges and the adjacent pebbles be smeared into a 3-D annulus shape for the core calculation and a 1-D spherical shape for the node spectrum calculation. The overall number densities for both the core and spectrum calculations must be preserved to yield the appropriate reaction rates. The fuel pebble structure for the spectrum calculation must also be maintained for proper resonance absorption, but extra graphite must be added to the shell region of the pebble model to account for the added thermalization of the graphite wedges. The wedge graphite was modeled as a large shell region on a single pebble as was done for the moderator pebbles in the pebble bed region as shown in Figure 11 where the actual geometry is indicated on the left while the 1-D Spherical geometry of the associated COMBINE model is shown on the right.
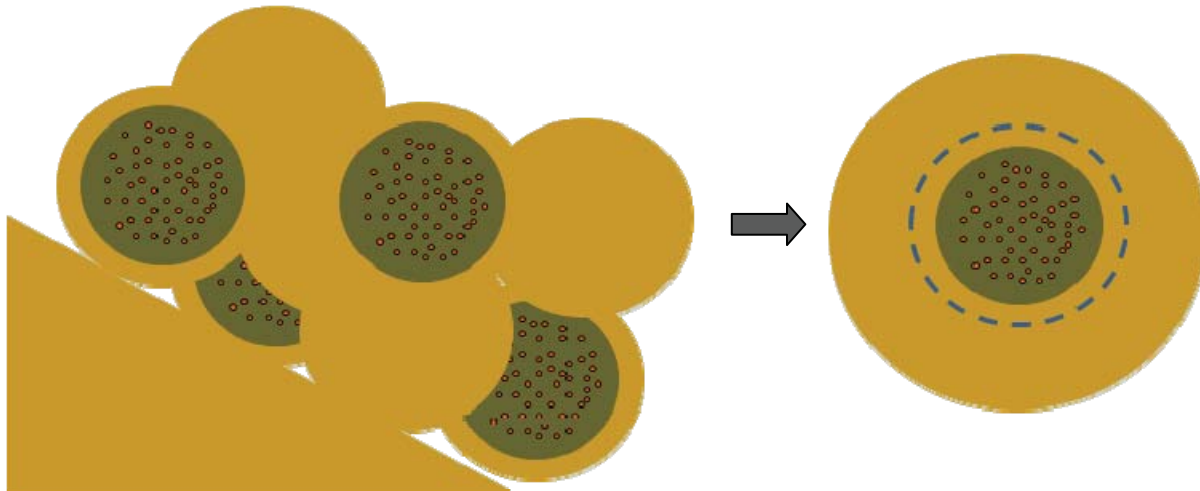
Figure 11. Homogenization of the pebble bed/lower reflector boundary zone.

3.3.7   Homogenization of the Control Rod Zones

The control rods are metallic tubes or bars lowered axially into the core. Because of the relatively strong absorption in these components, local scattering is not isotropic and absorption within them is not spatially uniform. Simply smearing the materials over the volume of the node retains the number densities but the microscopic cross sections will be inaccurate. A 1-D cylindrical transport model is thus solved with the explicit geometry of the control rod region to obtain the correct microscopic cross sections to use the zone-average number densities as shown in Figure 7. The tapered copper ACR was modeled as a solid cylinder with an equivalent area. The cross sectional area of the bar decreases over the height of the bar so the number density within a node was computed from the volumetric average. PEBBED constructs and executes a COMBINE model with this geometry and multiplies the resulting microscopic cross sections by the zone-averaged number densities to obtain the correct macroscopic cross sections for the node.

3.3.8   Homogenization of the Reflector Zones

Parts of the Proteus reflectors are pure graphite, perhaps with coolant holes drilled through them. Nodes with this composition are assumed to be homogeneous and no spatial transport calculation is performed—just a 'slowing-down' calculation for the homogenized medium. The top reflector, however, is supported by peralumen plates which have neutronic characteristics that differ from the graphite blocks they hold (Figure 12). The structure is actually more complex than indicated in the figure, but the simpler neutronically similar version shown was provided in the benchmark specification. 1-D cartesian models of the aluminum and graphite top reflector structures are built and executed by PEBBED to obtain properly homogenized reflector node cross sections.
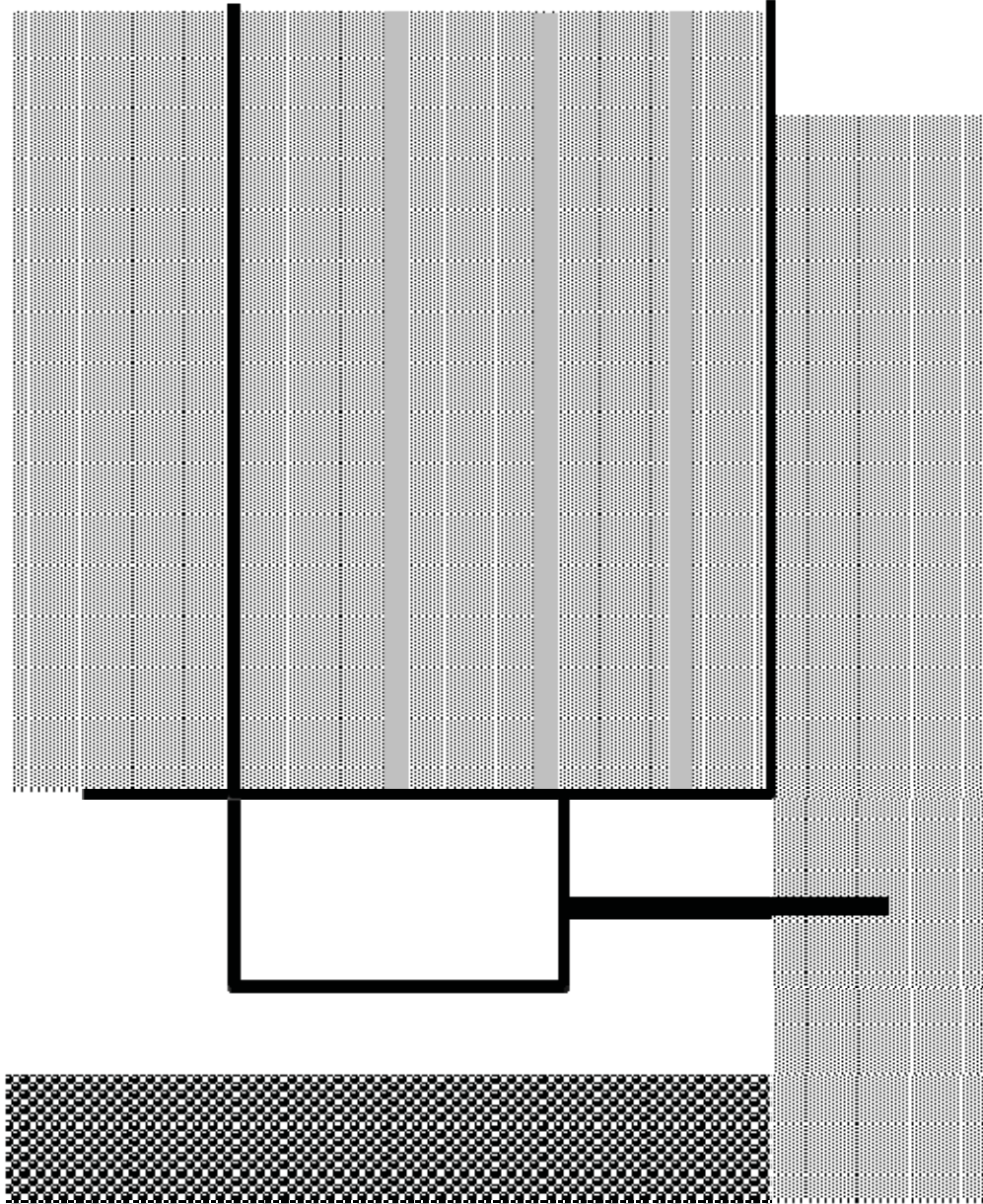
Figure 12. Simplified top reflector with peraluman support (black) structure holding graphite blocks.

3.4 Software

PEBDAN was developed at the Technical University of Delft, The Netherlands with support from INL. PEBDAN uses the core cavity dimensions and a spatial placement algorithm to compute a possible distribution of pebbles with the cavity. It then performs a Monte Carlo sampling of neutron tracks to obtain particle-level (INTRA) and pebble-level (INTER) Dancoff factors that explicitly takes into account the random distribution of these fuel lumps. The Dancoff factors are used by COMBINE to adjust the absorption rate in materials containing strong absorption resonances.

COMBINE Version 7.1 was used to generate multigroup diffusion and transport cross sections from ENDF/B v7 nuclear data libraries. It is still undergoing validation and verification and so the code used in this study is considered to be a 'beta' version. COMBINE is a portable B-1 or B-3 spectrum generation

code that exploits the Bondarenko and Nordheim Integral algorithms for neutron slowing-down in the resonance region. For direct computation of few-group diffusion constants, COMBINE 7.1 is called as a subroutine in PEBBED with local nuclide densities and temperatures written to COMBINE input files by PEBBED. This particular function of COMBINE and interface with PEBBED is similar to that employed in the previous analysis of Proteus Core 4.

The code was significantly altered in the modification from Version 7.0 to 7.1. The 1-D discrete ordinates transport code ANISN was embedded as a subroutine. The 1-D geometry of the region or component under study now must be included in the geometric specification with individual material compositions supplied for each major layer of the model. COMBINE performs a slowing down calculation for one or more of these layers and uses the converged flux spectra as the source for coalescing microscopic cross sections in the subsequent regions. These calculations are performed assuming white or specular boundary conditions (infinite medium). Once the cross sections have been generated for each layer, the 1-D S_n (Discrete Ordinates Scattering of Order n) transport equation is solved over the entire region. The microscopic cross sections for each layer are then updated using the leakage-corrected transport solution.

The other major upgrade to the code was the addition of an internal multiscale capability. For models with up to three layers of heterogeneity, such as particles embedded within pebbles, the sequence described in the preceding paragraph is performed sequentially with the homogenized microscopic cross sections at one scale (or stage) used in the subsequent stage. Coalescing into the final few group structure from the default 167 group COMBINE energy structure only occurs after the transport solution of the last stage is completed. In this manner, the highest possible fidelity is retained. In the previous study, COMBINE 0-D calculations were performed on the smeared pebble composition with only minor adjustments for thermal self-shielding. This calculation yielded 99-group cross sections for use in 1-D cylindrical SCAMP models of reactor core radial wedges. SCAMP is another 1-D discrete ordinates transport code developed at INL. The SCAMP calculations were used to coalesce and generate cross sections in the few-group structure for PEBBED. This captured the core level heterogeneity properly, but the detailed transport effects in the pebbles and control rods were not adequately captured.

Interzone leakage, which effects the slowing down spectrum, is provided by PEBBED as group-wise transverse buckling terms. For 0-D (homogeneous) compositions, the buckling is computed from the neutron leakages along all three dimensions. For 1-D COMBINE/ANISN models, only the transverse leakages are used to compute the buckling. COMBINE was written in FORTRAN 90 for execution on a Windows personal computer or on the high performance computing cluster.

PEBBED Version 5 solves the neutron diffusion and depletion equations in 1-D, 2-D, and 3-D and in Cartesian and cylindrical coordinates. Few-group cross sections are input manually or generated online with calls to COMBINE. To support the additional modeling capability of COMBINE 7.1, PEBBED was modified substantially to accept detailed specifications of multiply heterogeneous compositions such as pebbles, control rods, and reflector structures. For recirculating pebble bed cores with multiple pebble types and burnup levels, PEBBED constructs a fuel region unit cell from the average composition and geometry of the local pebble population. PEBBED runs on a Windows PC and on the high performance computing cluster. The archival version of PEBBED is maintained on the high performance computing cluster using the Tortoise Subversion version control software.

4. RESULTS AND INTERPRETATION

4.1 Dancoff Factor Calculation

Stochastically loaded pebble beds feature a variable packing density. The packing fraction tends to zero at the reflector where the pebbles maintain only point contact with the reflector walls. The packing fraction then oscillates, moving away from the wall. About 4 to 5 pebble diameters into the bed, the packing fraction shows only statistical variations. This profile, computed by the PEBDAN code, is shown in Figure 13.
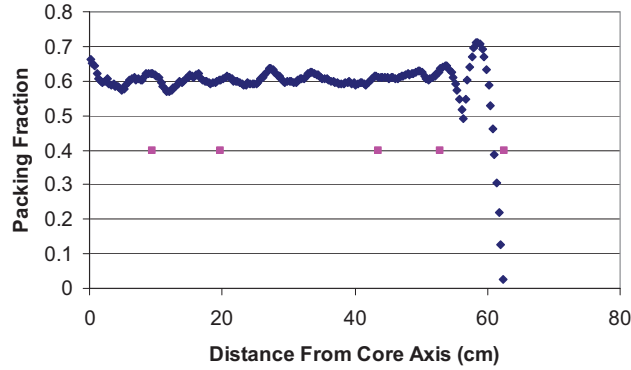
Figure 13. Radial variation in pebble packing fraction as computed by PEBDAN.

The magenta points in the diagram indicate only the location of the node radial boundaries chosen for this study. PEBDAN computes local packing fractions and Dancoff factors which were then averaged over each node to yield values for insertion into the COMBINE models. Figure 14 shows the variability of intrapebble and interpebble Dancoff factors in the radial and axial directions.
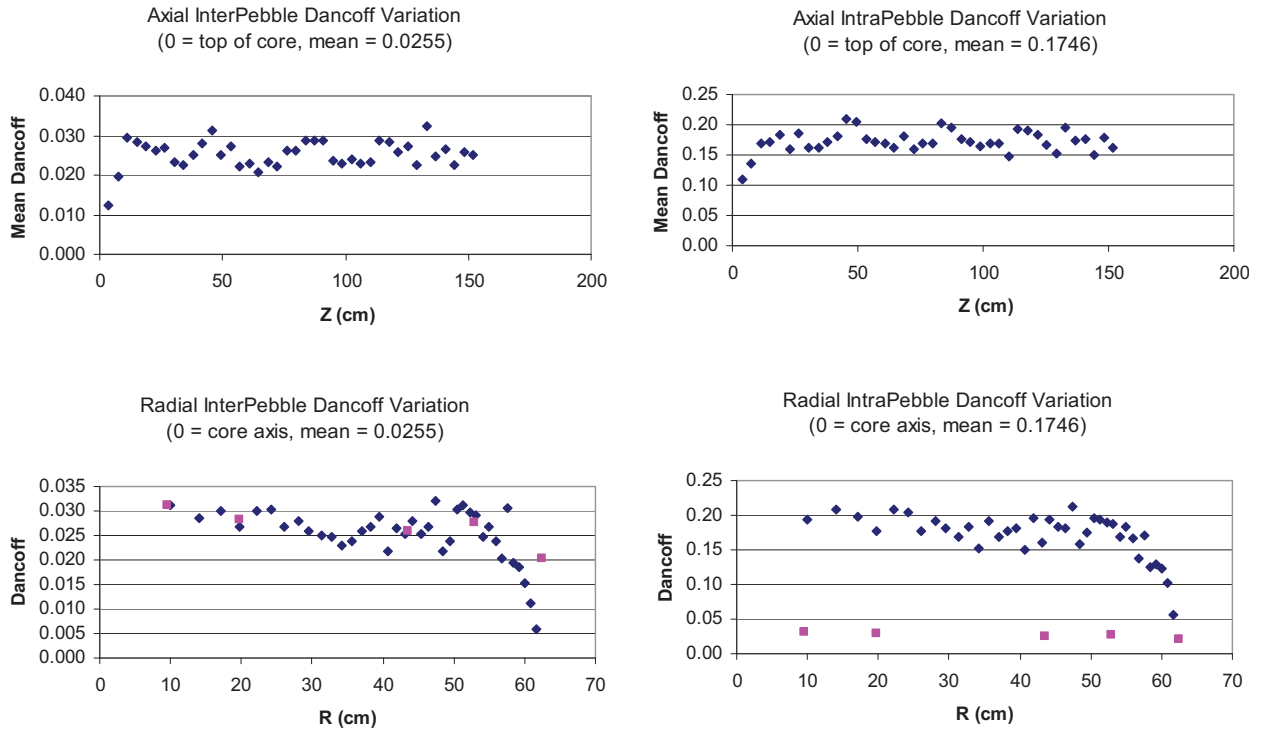
Figure 14. Dancoff factors along the radial and axial dimensions.

The Dancoff factors vary by about 20% along the axial dimension in the bulk of the core. The values drop off considerably near the top of the pebble bed (near the void), but as this is a region of low flux, this trend is not considered to be of consequence in the overall analysis. The radial variation in the values was considered to be significant enough to be reflected in the COMBINE calculations. For the purposes of the COMBINE spectrum analysis, the Dancoff factors were different for each radial channel (column) as shown in Table 3.

The mean packing fraction of the core equaled 0.5853, as determined experimentally from the mean bed volume and number of pebbles. The mean fraction computed from the PEBDAN calculation was 0.5839. There is no experimental data to validate the packing fraction variation in the Proteus core.

Table 3. Dancoff factor for the five radial zones.

Radius of Outer Boundary (cm)	Packing Fraction	Dancoff Factor	
		INTRA	INTER
9.5	0.6040	0.1938	0.0312
19.8	0.5991	0.1926	0.0283
43.5	0.6039	0.1777	0.0259
52.9	0.6154	0.1871	0.0277
62.5	0.5433	0.1394	0.0202

4.2 Eigenvalue Results for the RZ Core

Only computed core eigenvalues are compared here because no flux measurements were made in the Proteus core. For any reactor at steady state, the core eigenvalue is by definition equal to unity. The benchmark specification, however, omits a number of fine structural details that have an accumulated reactivity effect. This effect is estimated to be about +1.29% $\delta k/k$, which means that if the core specified in the benchmark is modeled with 100% energy and material fidelity, the computed eigenvalue would be 1.0129, not 1.000. All PEBBED error results are computed against this reference value.

Results were generated for six different cases assembled from two energy group's structures and assumptions about pebble packing fraction. Variation in the packing fraction of pebbles affects the neutronics in two ways: the first order effect is from the change in the number density of the isotopes; the second order effect is the change in the resonance shadowing by adjacent pebbles as reflected in the Dancoff factor. Since the relative and absolute magnitude of the effects is of interest, three cases were run for each energy group structure: (1) uniform packing density and Dancoff factor, (2) variable packing density with a constant Dancoff factor, and (3) variation in both packing density and the corresponding Dancoff factor. The results are shown in Table 4, which also includes the corresponding result from the PEBBED-COMBINE study of 2008.

Table 4. Eigenvalue results for different modeling assumptions.

CASE	k_{eff} (% $\delta k/k$)	
	1.0129	
Experimental (with benchmark bias)	4 group	16 group
Homogeneous packing fraction and Dancoff factor	1.0325 (1.9)	1.0318 (1.9)
Variable packing fraction, constant Dancoff factor	1.0300 (1.7)	1.0382 (2.5)
Variable packing fraction and Dancoff factor	1.0290 (1.6)	1.0366 (2.3)
Homogeneous packing fraction and Dancoff factor (previous study)	0.9588 (-5.3)	1.049 (-5.3)

Overall, the results indicate that the current modeling technique and code over-predict k_{eff} by 1.6 to 2.5%. Compared to high fidelity Monte Carlo analyses, this is quite large for eigenvalue predictions Higher errors are to be expected with this modeling approach, but a reduction in error can likely be achieved with further refinements and corrections to the model. When compared with the results from the 2008 analysis, the recent improvements to the COMBINE code moved the result in the right direction.

The four-group models yielded better eigenvalues than the comparable 16-group in the variable packing cases. This can reasonably be attributed to a cancellation of errors. A full energy group structure sensitivity study must be performed to reach any firm conclusions from this result.

The effect of variations in the peaking fraction is a bit more pronounced in the four-group case than in the 16-group case. Including variability in the model reduced the error in the four-group model from 1.9 to 1.6% with the change in number density accounting for most of the change as expected. Interestingly, the error in the 16-group models increased from 1.9 to 2.3% with no discernible trend emerging from these few data points. The lack of a trend suggests some canceling of errors that should be investigated further. The 16-group cases were observed to be rather sensitive to the choice of thermal-fast boundary (set in the PEBBED input). A proper sensitivity study must be performed to obtain any firm conclusions from this data.

Table 5 and Table 6 show the peak fast and thermal fluxes generated by the different models. The coarser four-group structure shows slightly more peaking in the fast flux. The thermal peaking is comparable. Similarly, assuming the variability in the packing fraction as predicted by PEBDAN yields a slightly peak fast flux, but the <1% difference would not be of safety significance in a power reactor.

Table 5. Comparison of peak fast (>1.9 eV) flux.

CASE	Peak Fast Flux*	
	4 group	16 group
Homogeneous packing fraction and Dancoff factor	7.18E+13	6.92E+13
Variable packing fraction, constant Dancoff factor	7.23E+13	6.97E+13
Variable packing fraction and Dancoff factor	7.24E+13	7.04E+13

* Based on core fission power of 5 MW.

Table 6. Comparison of peak thermal (<1.9 eV) flux.

CASE	Peak Thermal Flux*	
	4 group	16 group
Homogeneous Packing Fraction and Dancoff Factor	5.23E+13	5.20E+13
Variable Packing Fraction, Constant Dancoff factor	5.18E+13	5.19E+13
Variable Packing Fraction and Dancoff Factor	5.19E+13	5.22E+13

* Based on core fission power of 5 MW.

4.3   Comparison of Flux Profiles as Computed by PEBBED and COMBINE/ANISN

A comparison of flux profiles was not performed for multidimensional models because a comparable multidimensional transport model of PROTEUS Core 4.2 has not yet been performed. A 3-D MCNP calculation is being concluded by INL, but for the other Proteus cores which featured pebbles loaded in a crystalline lattice. It is not obvious how those results could be compared usefully to the PEBBED profiles.

Flux profiles can be compared, however, between PEBBED (diffusion) and the ANISN transport solutions used to generate the cross sections. Given the high error values in the core multiplication value, it is useful to compare these results to see where inconsistencies may exist.

To achieve a useful comparison, the RZ model of the Proteus core was simplified to include a single, unreflected fuel layer in the axial dimension with purely reflective boundary conditions and an azimuthally uniform control rod curtain. This effectively eliminates all axial and azimuthal leakage, making the core, in effect, an infinite reflected cylinder with a control rod in the side reflector. Under these conditions, the PEBBED and ANISN 1-D radial flux profiles should match very well.

A 16-group model with variable packing fraction was built and executed for this core. The fast group fluxes out through the concrete shield were plotted in Figure 15 and the corresponding thermal group fluxes were plotted in Figure 16. Because the flux changes by many order of magnitude over this range, a logarithmic axis was used. The fluxes were normalized to the average fission power to facilitate comparison. The transport fluxes were plotted with solid lines while the corresponding diffusion fluxes were plotted with individual points. The orange-shaded region is the core and the green region is the control rod node.
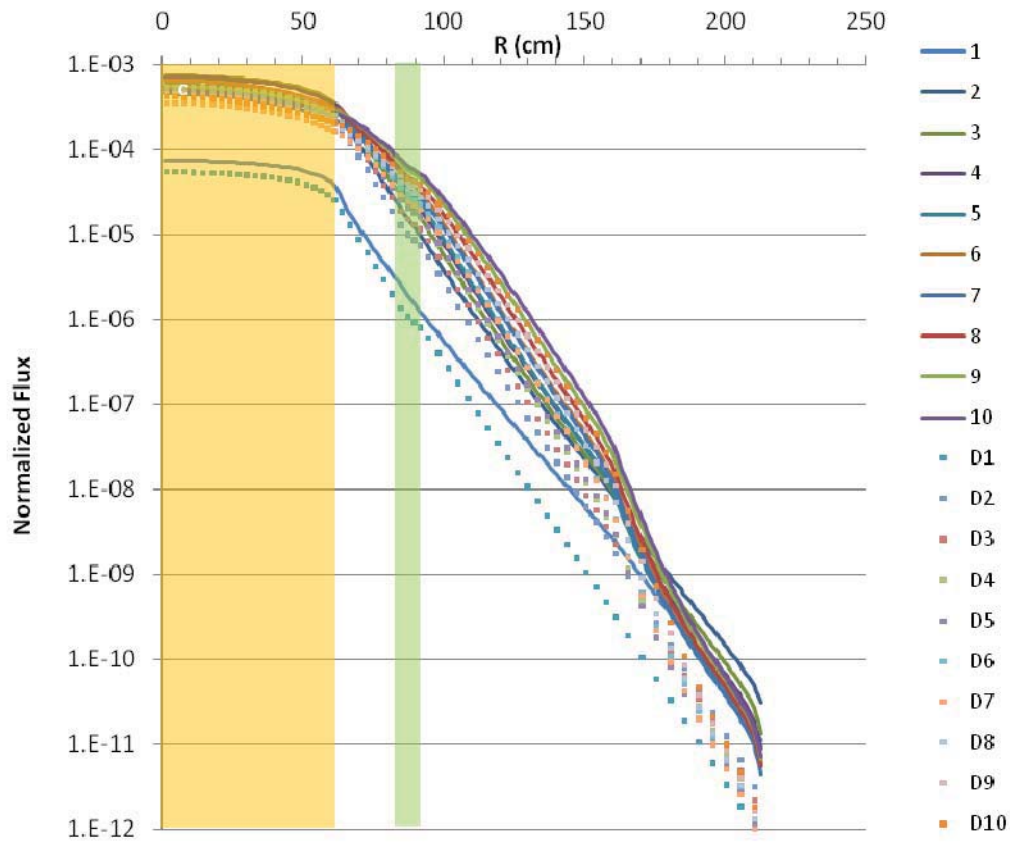
Figure 15. Group-wise fast flux radial profile—diffusion vs. transport.
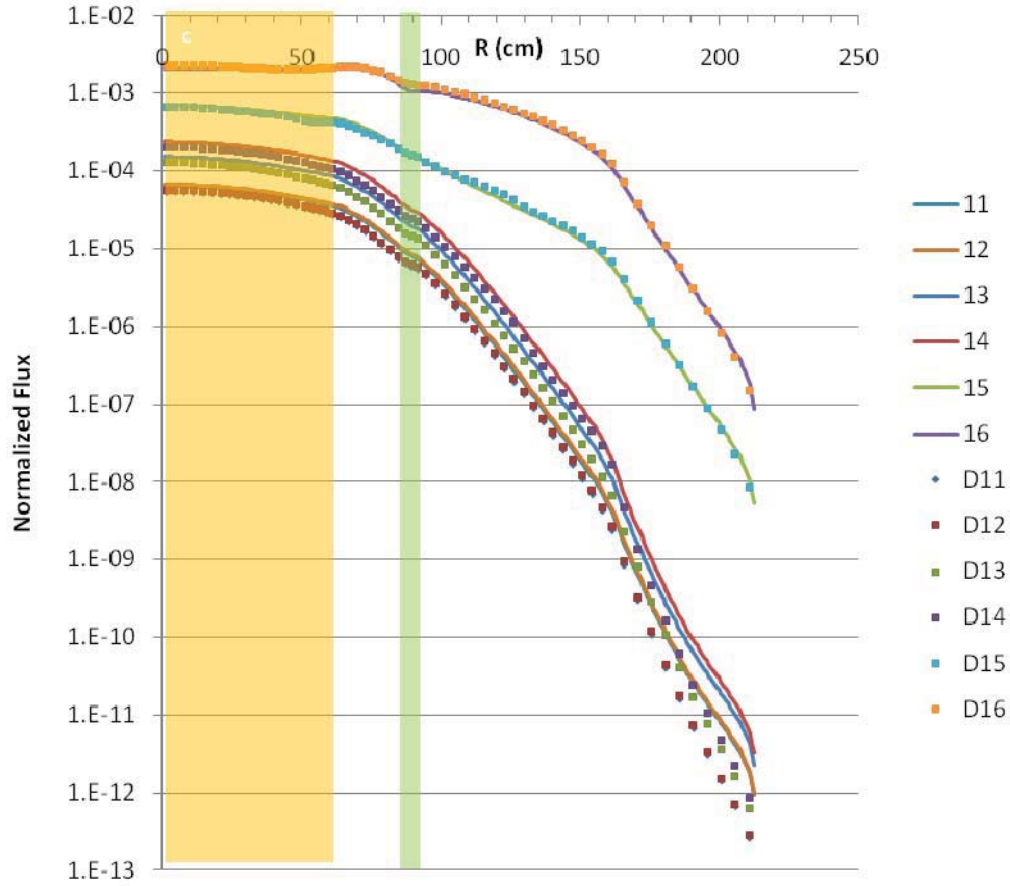
Figure 16. Group-wise thermal flux radial profile—diffusion vs. transport.

Through the core and into the side reflector, the fluxes appear to agree quite well, particularly for the thermal fluxes. Diffusion theory under-predicts the fast flux far from the core; a known deficiency of the diffusion approximation.

A log plot, however, can hide differences over a shorter range. The flux values, therefore, were plotted on a linear scale from the core center out through the control rod only (Figure 17 and Figure 18). Significant differences are observed between the transport and diffusion solutions in the lowest energy group (0 to 0.12 eV) both in the pebble bed core itself and in the control rod node. Because this group also has the largest fission cross section, the power generated by these slow neutrons is a large fraction of the total and thus the power normalization factor is strongly affected by changes in this group flux. While the other thermal flux profiles agree quite well, the fast flux profiles computed by diffusion theory are all biased downward because of the elevated thermal power of the lowest group.

The cause of the discrepancy in the lowest group is being investigated, but a difference of this magnitude certainly can account for the 1 to 2% difference in the core multiplication factor. A positive thermal flux error would translate into a positive neutron source error and thus a high value for k_{eff}. The cause of the error in the lowest group observed within the pebble bed region may also be responsible for the over-prediction of the very low thermal flux in the control rod zone. Alternatively, an over-prediction of the thermal flux in the control rod will cause an elevated flux in the pebble bed region (and a high k_{eff}) . This higher thermal flux will generate a higher power normalization factor that will lower the fast flux profiles as indicated in Figure 17.
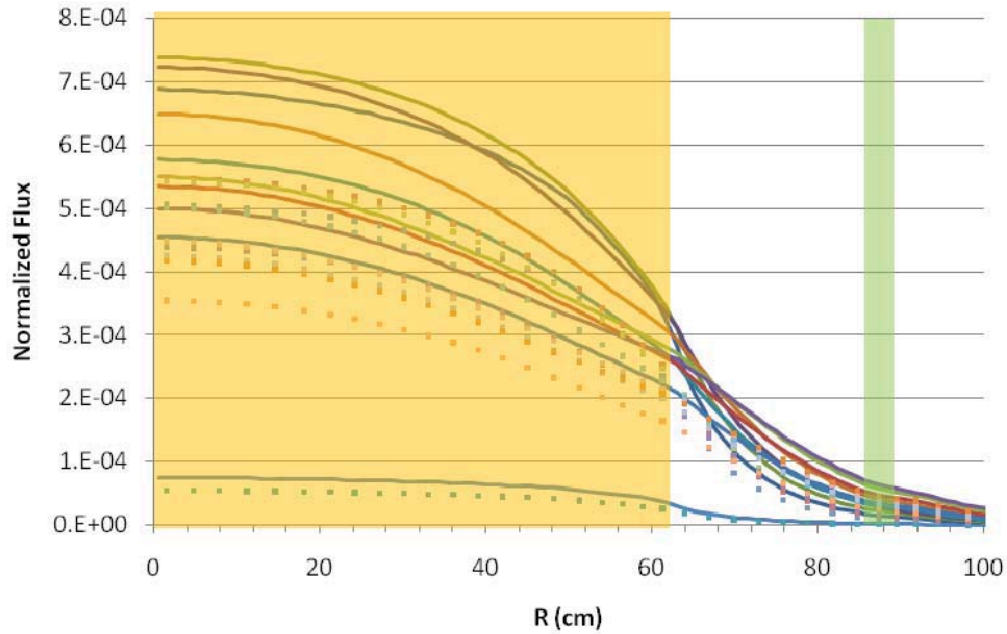
Figure 17. Group-wise fast flux through the core and control rod regions.
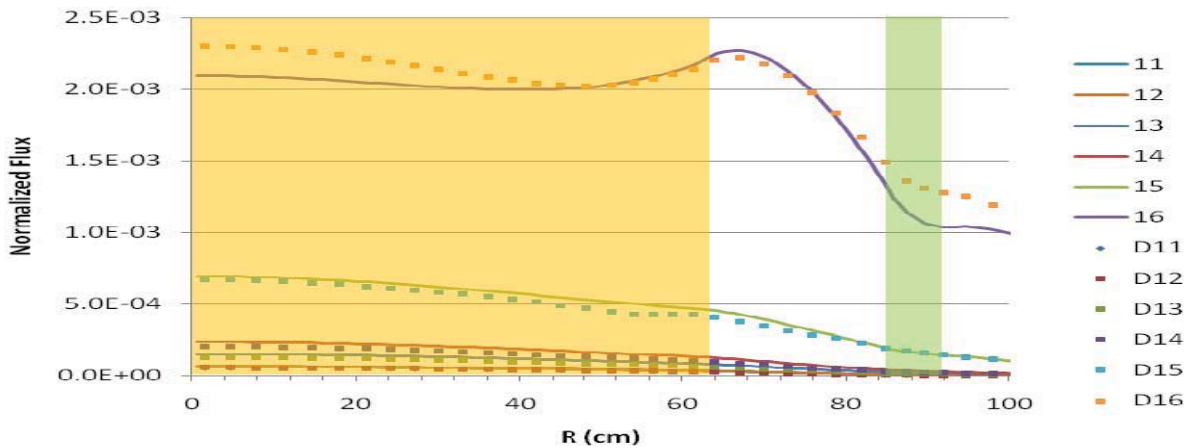
Figure 18. Group-wise thermal flux through the core and control rod regions.

One possible source of the discrepancy is the diffusion coefficient generated by COMBINE. Diffusion coefficients are not used in solving the transport equation but are derived from transport theory using simplifying assumptions and approximations (e.g., Fick's Law of Diffusion or P1 theory). As discussed in Section 3.2, the normal cross section homogenization process does not preserve leakages between pebbles, and the diffusion coefficients must be adjusted using a semi-empirical method. This adjustment is dependent upon energy and is particularly pronounced in the thermal region. The proper definition of the diffusion coefficient will be derived in the coming months to yield acceptable agreement with transport theory for pebble beds and in the absorber regions. Another possible source of the error is the homogenization of the control rod node. This is a difficult process in that one must be careful to preserve the geometry of the rods when generating microscopic cross sections while using the average nuclide densities (smeared over volume of the control rod annulus) to obtain the correct reaction rates. This procedure must be reviewed.

4.3.1 General Observations and Recommendations

Observations from this study include:

- Recent improvements in the COMBINE code, mainly the use of 1-D transport to model the fine detail of the pebbles for cross section homogenization, significantly reduced the error in core neutronic calculations. The error in the core multiplication factor , however, is still on the order of 2 to 2.5%, unacceptably high for a production code. Incorrect modeling assumptions may also be at fault.

- There is a large discrepancy in the lowest energy thermal flux between transport theory and diffusion theory when the transport calculation is used to derive the diffusion theory parameters. Since the same absorption and fission cross sections are used in the transport and diffusion calculations, a possible source of the error is in the derivation or calculation of diffusion coefficients from the transport solution.

- Explicit modeling of variations in the pebble packing fraction improves the solution to a small extent, but neglecting this effect does not significantly impact the whole core calculation when compared to other possible sources of error.

4.3.2 Gaps and Proposed Remediation

In the previous analysis of the Proteus Core using PEBBED and an older version of COMBINE, a number of recommendations were made to improve the ability to accurately model pebble bed core neutronics with INL's deterministic codes. The recommendations from that study are listed here with a status report on their implementation.

- *Develop a randomly packed unit cell model with MCNP for confirming COMBINE calculations.*

  This was performed and will be the subject of a separate INL report describing the validation and verification of the multiscale COMBINE code. Selected results for a unit cell pebble shown in this report indicate that COM BINE calculations agree well with MCNP and other methods of modeling the neutronics of a pebble.

- *Confirm and correctly implement an interpebble streaming correction.*

  The streaming correction was implemented within COMBINE. Test results will be included in the report mentioned in the previous bullet.

- *Confirm and correctly implement a void treatment.*

  The calculation of effective diffusion coefficients for the void space above the PBR proposed by Gerwin and Scherer[18] was employed in this study, but the accuracy has not yet been independently confirmed. The effect on core calculations is not as significant as other phenomenon so this task has not received a high priority.

- *Model local packing/Dancoff variations.*

  This was addressed directly in this study. Modeling these variations improves the result but the improvement does not significantly impact core safety parameters.

- *Implement a proper cross section generation model using 1-D radial transport solutions.*

  This was completed and demonstrated in this study. The results of unit cell calculations of a single pebble indicate that this approach works well, except for the lowest thermal energy range. The definition and calculation of diffusion coefficients at very low energies may be the source of the discrepancy and will be investigated in the coming months.

- *Develop and implement a decent control rod treatment.*

  Efforts continue in this area. The multiscale capabilities of COMBINE allow for explicit transport treatment of a cylindrical control rod assembly in PEBBED. Results indicate that this treatment is accurate except in the lowest thermal region. This discrepancy coincides with that of the low energy thermal flux predicted in the pebble bed itself and thus may be resolved along with this issue. The use of discontinuity factors derived using Generalized Equivalence Theory (as is traditionally done in LWR nodal core simulation) may also yield improvements. INL is also developing an approach that employs transport-derived response functions for accurate multidimensional modeling of control rods. This method is in the advanced stages of development and testing.

- *Develop a multiscale cross section generation algorithm in which TRISO particles are modeled explicitly rather than smeared and corrected using approximate techniques.*

  Done and employed in this study.

- *All future code modifications and upgrades must be validated with PROTEUS or other real benchmark data.*

  This Proteus benchmark provides a suitable test for validating PEBBED and other pebble bed modeling tools and techniques.

  In addition to the remaining issues to be resolved, the implementation of 3-D modeling capability must be fixed. The issues associated with memory and file input and output should be resolved in the coming months.

5. SUMMARY

This study was the second attempt to validate the INL deterministic pebble bed analysis tools and the first investigation of the accuracy of the multiscale transport capability implemented in COMBINE. The results from whole core neutronic model analyses indicate a significant improvement over the previous version of COMBINE, but that further improvements are needed. A correct coalescing of low energy diffusion theory parameters from COMBINE/ANISN transport results should reduce the error in core eigenvalue results from 2 to 2.5% δk/k to a more acceptable level.

Variations in packing fraction were tested in this study. The variations affect the local isotopic number densities and, to a lesser extent, the resonance absorption rate as reflected in the Dancoff factor. Explicitly modeling these variations improves the prediction of k_{eff}, but the magnitude of the improvement is minor.

The ability to model PBR cores with a diffusion-based core simulator has been improved, but a few final corrections and testing are required for these codes to yield the high fidelity results needed for reliable core analysis. These corrections should be completed within the coming fiscal year.

6.   COMPUTER HARDWARE, SOFTWARE, AND MODELS

6.1   Hardware

All computations in this study were performed on a Dell Precision M6300 portable workstation. This computer features an Intel Core 2 Duo processing unit running at 2.50 GHz with 8 GB of random access memory and the Microsoft Windows XP Professional x64 version 2003operaitng system.

6.2   Software

PEBBED Release 428 was used for all core simulations. The stand-alone beta version 1g of COMBINE 7.1, released on April 26, 2010, was modified to be called as a subroutine within PEBBED. COMBINE 7.1 is released with the nuclear data libraries matxs.lib and reres.lib. The PEBDAN code has no version number.

6.3   Models

Table 7 lists the PEBBED input decks that were constructed and executed for this study.

Table 7. PEBBED input decks constructed and executed for this study.

PEBBED Filename	# of Groups	Control Node	Dimensionality	Pebble Packing
LP4_4gRZ_ACR*	4	ACR only	2D (RZ)	Homogeneous
LP4_16gRZ_ACR*	16	ACR only	2D (RZ)	Homogeneous
LP4_4gRZBCR_het	4	ACR/WCR hybrid	2D (RZ)	Variable density and Dancoff factor
LP4_16gRZBCR_het**	16	ACR/ WCR hybrid	2D (RZ)	Variable density and Dancoff factor
LP4_4gRZBCR_homdan	4	ACR/ WCR hybrid	2D (RZ)	Variable density but constant Dancoff factor
LP4_16gRZBCR_homdan	16	ACR/ WCR hybrid	2D (RZ)	Variable density but constant Dancoff factor
LP4_4gRZBCR_hom	4	ACR/ WCR hybrid	2D (RZ)	Homogeneous
LP4_16gRZBCR_hom	16	ACR/ WCR hybrid	2D (RZ)	Homogeneous
LP4_4g3D	4	Explicit - separate ACR and WCR	3D (RθZ)	Variable density and Dancoff factor
LP4_16g3D	16	Explicit - separate ACR and WCR	3D (RθZ)	Variable density and Dancoff factor

*   Used to generate microscopic cross sections for the copper and aluminum components of the ACR. These cross sections are used in the hybrid BCR models.

**   Included in Appendix A, Section A-2.

7. REFERENCES

1. Terry, W. K., H. D. Gougar, and A. M. Ougouag, "Direct Deterministic Method for Neutronics Analysis and Computation of Asymptotic Burnup Distribution in a Recirculating Pebble-Bed Reactor," *Annals of Nuclear Energy*, Vol. 29, 2002, pp. 1345–1364.

2. Hiruta, H., et al, "CYNOD: A Neutronics Code for Pebble Bed Modular Reactor Coupled Transient Analysis," INL/CON-08-14160, September 2008.

3. Gougar, H., Ougouag, A, and Terry, W. "Validation of the Neutronic Solver within the PEBBED Code for Pebble Bed Reactor Design," Proceedings of the M&C 2005: International Topical Meeting on Mathematics and Computation, Avignon, France.

4. Gougar, H., Reitsma, F., and Joubert, W. "A Comparison of Pebble Mixing and Depletion Algorithms Used in Pebble-Bed Reactor Equilibrium Cycle Simulation," *Proceedings of the M&C 2009: International Topical Meeting on Mathematics and Computation, Saratoga Springs, NY.*

5. International Atomic Energy Agency, *Critical Experiments and Reactor Physics Calculations for Low-Enriched High Temperature Gas Cooled Reactors,* IAEA-TECDOC-1249, Vienna, 2001.

6 . Gougar, H, *Results of a Neutronic Simulatin of HTR-Proteus Core 4.2 Using PEBBED and Other INL Reactor Physics Tools: FY-09 Report*, INL/EXT-09-16620, August 2009.

7. T. Williams, "LEU-HTR-Proteus: Configuration Descriptions and Critical Balances for the Cores of the HTR-Proteus Experimental Programme," TM-41-95-18 (Version 1), Paul Scherrer Institut, 25 November 1996.

8. D. Mathews and T. Williams, "LEU-HTR-Proteus System Component Description," TM-41-93-43 (version 2), Paul Scherrer Institut, 25 November 1996.

9. W. Terry, A. Wemple, B. Dolphin, *Evaluation of the HTR-Proteus Pebble Bed Reactor Experiments*, INL/EXT -89-14768, Rev 20, August 2009.

10. F. Reitsma, "The Pebble Bed Modular Reactor Layout and Neutronics Design of the Equilibrium Cycle," Proceedings of PHYSOR 2004—The Physics of Fuel Cycles and Advanced Nuclear Systems: Global Developments, *American Nuclear Society Topical Meeting, Chicago, IL, April 25-29, 2004*.

11. Bess, J. D., and N. Fujimoto, "Evaluation of the Start-Up Core Physics Tests at Japan's High Temperature Engineering Test Reactor (Fully Loaded Core)," HTTR-GCR-RESR-001, *International Handbook of Evaluated Reactor Physics Benchmark Experiments*, NEA/NSC/DOC(2006)1, OECD-NEA, March 2009.

12. Goto, Minoru, et al., 2006, "Neutronics Calculations of HTTR with Several Nuclear Data Libraries," *J. Nuc. Scien. Tech.*, Vol. 43, N. 10, pp. 1237–1244.

13. J. Ortensi, J. Cogliati, M. Pope, J. Bess, M. Ferrer, A. Bingham, and A. Ougouag, *Deterministic Modeling of the High Temperature Test Reactor*, INL/EXT-10-18969, June 2010,

14. DOE-HTGR-90406*, MHTGR Nuclear Physics Benchmarks,* General Atomics, 1994.

15. W. Yoon, R. Grimesey, D. Nigg, and R. Curtis, *COMBINE7.0 – A Portable ENDF/B-VII.0 Based Neutron Spectrum and Cross-Section Generation Program*, INL-EXT-08-14729, September 2008.

16. Kloosterman, J. L. and Ougouag, A. M., "Spatial Effects in Dancoff Factor Calculations for Pebble-Bed HTRs," *Proceedings of the American Nuclear Society Topical Meeting on Mathematics and*

Computation, Supercomputing, Reactor Physics and Nuclear and Biological Applications, Palais des Papes, Avignon, France, September 12–15, 2005.

17. Lieberoth, J. and Stojadinović, A., "Neutron Streaming in Pebble Beds," *Nuclear Science and Engineering*: Vol. 76, 1980, pp. 336–344.

18. H. Gerwin and W. Scherer, "Treatment of the Upper Cavity in a Pebble-Bed High-Temperature Gas-Cooled Reactor by Diffusion Theory," *Nuclear Science and Engineering,* Vol. 97, 1987, pp. 9–19

19. G Hosking, T D Newton, O Kberl, P Morris, S Goluoglu, T Tombakoglu, U Colak & E Sartori, "Analysis of an OECD/NEA High-Temperature Reactor Benchmark", Proc PHYSOR 2006, Vancouver, Canada, September 2006.

Appendix A

Referenced Figures/Tables

Appendix A—Referenced Figures/Tables

A-1. Figures and Tables
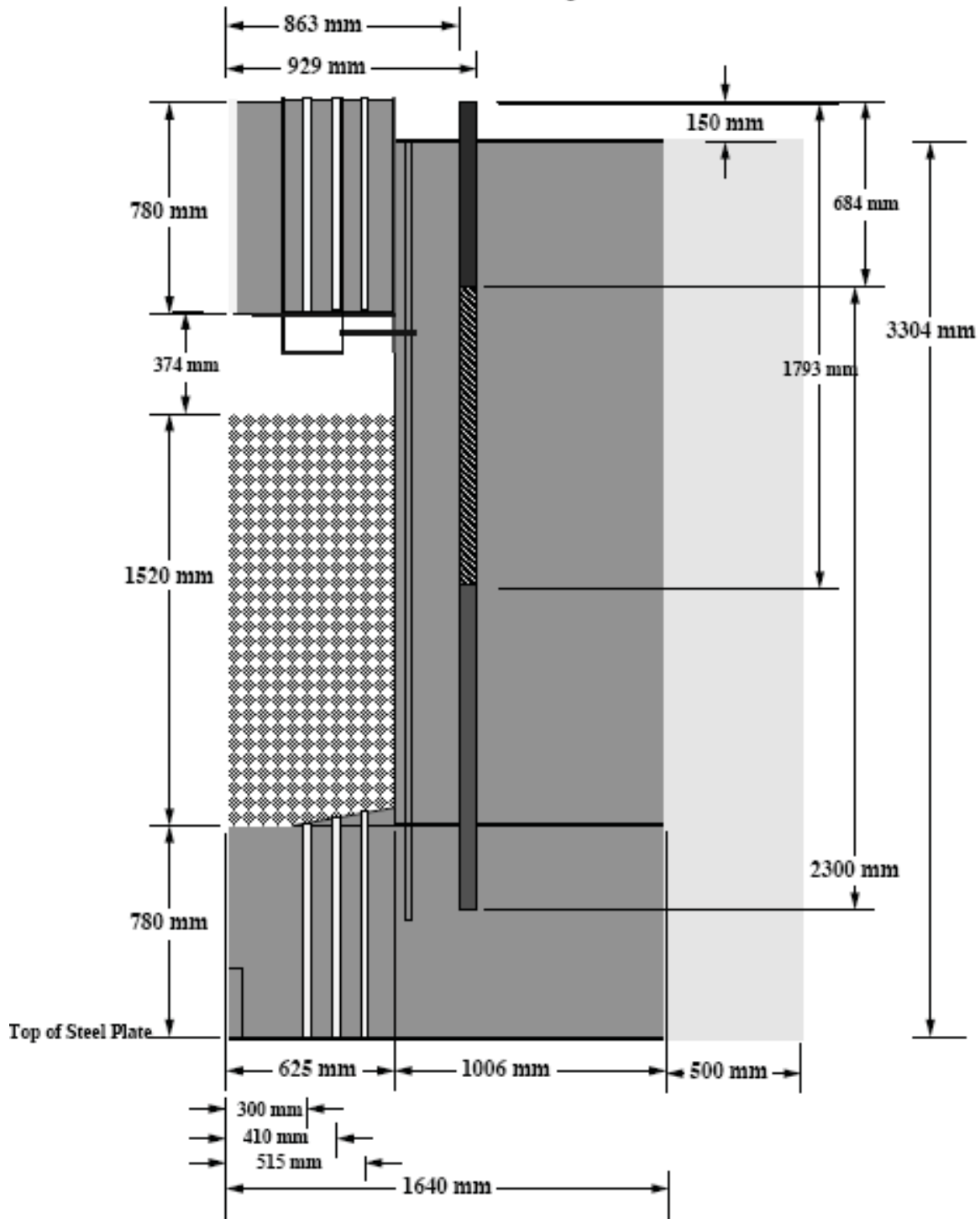
Figure A-1. Detailed RZ geometry of Proteus core 4.2

Table A-1. Material assignment in the RZ model.

Mesh subdivision

			9.5	19.8	43.5	52.9	62.5	86.25	92.85	128	163.1	213.1
			1	1	1	1	1	1	1	1	1	1
		0	9.5	10.3	23.7	9.4	9.6	23.75	6.6	35.15	35.1	50
15.0	1	15	32	9	26	32	28	33	45	33	33	29
42.4	1	27.4	32	9	26	32	28	9	10	9	9	29
68.4	1	26	32	9	26	32	28	9	10	9	9	29
78.4	1	10	32	24	25	25	25	9	11	9	9	29
94.3	1	15.9	42	42	27	43	43	44	12	9	9	29
115.4	1	21.1	42	42	42	42	42	9	13	9	9	29
130.4	1	15	1	1	1	1	1	9	14	9	9	29
152.3	1	21.9	1	1	1	1	1	9	15	9	9	29
179.3	1	27	1	1	1	1	1	9	16	9	9	29
206.0	1	26.7	1	1	1	1	1	9	17	9	9	29
226.9	1	20.9	1	1	1	1	1	9	18	9	9	29
247.4	1	20.5	1	1	1	1	1	9	19	9	9	29
259.4	1	12	1	1	1	1	1	9	20	9	9	29
267.4	1	8	1	1	6	7	8	9	21	9	9	29
286.4	1	19	9	9	31	32	9	9	22	9	9	29
298.4	1	12	9	9	31	32	9	9	23	9	9	29
315.4	1	17	9	9	31	32	9	9	9	9	9	29
333.4	1	18	9	9	31	32	9	9	9	9	9	29
345.4	1	12	9	9	31	32	9	9	9	9	9	29

COMPOSITIONS

1	Core Radial Zone 1	15	BCR	31	CHR1,2 (Lower reflector)
2	Core Radial Zone 1	16	ACR10	32	Lower reflector CHR3
3	Core Radial Zone 1	17	ACR11	33	Ref Void
4	Core Radial Zone 1	18	ACR12	34	CR_Hole
5	Core Radial Zone 1	19	ACR13	35	ACR4
6	Core/Ref Wedge 4	20	ACR14	36	ACR5
7	Core/Ref Wedge 5	21	ACR15	37	ACR6
8	Core/Ref Wedge 6	22	ACR16	38	ACR7
9	Pure Graphite Reflector	23	Al/C/Air Top Reflector 1	39	ACR8
10	WCRinCore	24	Al/C/Air Top Reflector 2	40	ACR9
11	BCR	25	Al/C/Air Top Reflector 3	41	Above ACR
12	BCR	26	TopVoidAl	42	TopVoid
13	BCR	27	Al/C/Air Top Reflector 5	43	TopVoidAl2
14	BCR	28	Concrete	44	RefAl
15	BCR	30	Air	45	WCRexCore

Table A-2. Number densities for pebbles.

Material Balance					Kernel		Fuel Zone		Pebble	
Element	Isotope	wt.frac	atom frac	comp a/f*	mass (g)	N (#/bn-cc)	mass(g)	N (#/bn-cc)	mass(g)	N (#/bn-cc)
Pu						**0.0000E+00**				
	Pu238	0.0000E+00	0.0000E+00		0.00000E+00	0.00000E+00	0.00000E+00	0.00000E+00	0.00000E+00	0.00000E+00
	Pu239	0.0000E+00	0.0000E+00		0.00000E+00	0.00000E+00	0.00000E+00	0.00000E+00	0.00000E+00	0.00000E+00
	Pu240	0.0000E+00	0.0000E+00		0.00000E+00	0.00000E+00	0.00000E+00	0.00000E+00	0.00000E+00	0.00000E+00
	Pu241	0.0000E+00	0.0000E+00		0.00000E+00	0.00000E+00	0.00000E+00	0.00000E+00	0.00000E+00	0.00000E+00
	Pu242	0.0000E+00	0.0000E+00		0.00000E+00	0.00000E+00	0.00000E+00	0.00000E+00	0.00000E+00	0.00000E+00
U				comp a/f*		**2.43618E-02**				
	U235	0.1674	1.6901E-01	0.1692	1.06444E-04	4.11729E-03	9.99931E-01	4.71281E-05	9.99931E-01	2.26527E-05
	U238	0.8313	8.2878E-01	0.8295	5.28662E-04	2.01906E-02	4.96625E+00	2.31109E-04	4.96625E+00	1.11085E-04
	U234	0.0014	1.3710E-03	1.2923E-03	8.59799E-07	3.34000E-05	8.07696E-03	3.82309E-07	8.07696E-03	1.83761E-07
	U233	0.0000	0.0000E+00		0.00000E+00	0.00000E+00	0.00000E+00	0.00000E+00	0.00000E+00	0.00000E+00
	U236	0.0000	8.4148E-04		5.32241E-07	2.05000E-05	4.99888E-03	2.34651E-07	4.99888E-03	1.12788E-07
Th						**0.00000E+00**		0.00000E+00		0.00000E+00
	Th232	0	1		0.00000E+00	0.00000E+00	0.00000E+00	0.00000E+00	0.00000E+00	0.00000E+00
Si						**0.00000E+00**		**5.89994E-04**		**2.83588E-04**
	Si28	0	0		0.00000E+00	0.00000E+00	1.37423E+00	5.44151E-04	1.37423E+00	2.61553E-04
	Si29	0	0		0.00000E+00	0.00000E+00	7.22701E-02	2.76294E-05	7.22701E-02	1.32804E-05
	Si30 *	0	0		0.00000E+00	0.00000E+00	4.92795E-02	1.82131E-05	4.92795E-02	8.75435E-06
C						**0.00000E+00**		**8.46834E-02**		**8.56050E-02**
	C12	0	0		0.00000E+00	0.00000E+00	9.07138E+01	8.37434E-02	1.90781E+02	8.46548E-02
	C13	0	0		0.00000E+00	0.00000E+00	1.10336E+00	9.39986E-04	2.32048E+00	9.50215E-04
B				2.86551E-10		**0.00000E+00**		**3.70614E-08**		**3.73173E-08**
	B10	0.000000	0.000000		0.00000E+00	0.00000E+00	6.63269E-06	7.33815E-09	1.38944E-05	7.38883E-09
	B11	0.000000	0.000000		0.00000E+00	0.00000E+00	2.95391E-05	2.97232E-08	6.18794E-05	2.99285E-08
O				4.8724E-02		**4.86157E-02**		**5.56474E-04**		**2.67476E-04**
	O16	0.99734626	0.99762		8.53262E-05	4.85000E-02	8.01554E-01	5.55149E-04	8.01554E-01	2.66839E-04
	O17	0.00040375	0.00038		3.45419E-08	1.84740E-05	3.24486E-04	2.11460E-07	3.24486E-04	1.01641E-07
	O18	0.00224999	0.002		1.92494E-07	9.72314E-05	1.80829E-03	1.11295E-06	1.80829E-03	5.34952E-07
He						**0.00000E+00**		0.00000E+00		0.00000E+00
	He3	0	0		0.00000E+00	0.00000E+00	0.00000E+00	0.00000E+00	0.00000E+00	0.00000E+00
	He4	0	0		0.00000E+00	0.00000E+00	0.00000E+00	0.00000E+00	0.00000E+00	0.00000E+00
H	H1				0.00000E+00	0.00000E+00	0.00000E+00	0.00000E+00	0.00000E+00	0.00000E+00
N	N14				0.00000E+00	0.00000E+00	0.00000E+00	0.00000E+00	0.00000E+00	0.00000E+00

Table A-3. Number densities for reflector and wedge nodes.

Nom Unit Cell		Reflector	Wedge3	Wedge4	Wedge5
		1	0.26118434	5.6865E-01	0.720736534
mass(g)	N (#/bn-cc)		0.707324445	8.3411E-01	0.872448101
			N (#/bn-cc)		
0.00000E+00	0.00000E+00		0.00000E+00	0.00000E+00	0.00000E+00
0.00000E+00	0.00000E+00		0.00000E+00	0.00000E+00	0.00000E+00
0.00000E+00	0.00000E+00		0.00000E+00	0.00000E+00	0.00000E+00
0.00000E+00	0.00000E+00		0.00000E+00	0.00000E+00	0.00000E+00
0.00000E+00	0.00000E+00		0.00000E+00	0.00000E+00	0.00000E+00
4.99965E-01	6.83892E-06		5.05270E-06	2.94994E-06	1.90986E-06
2.48312E+00	3.35371E-05		2.47777E-05	1.44661E-05	9.36568E-06
4.03848E-03	5.54782E-08		4.09882E-08	2.39303E-08	1.54930E-08
0.00000E+00	0.00000E+00		0.00000E+00	0.00000E+00	0.00000E+00
2.49994E-03	3.40510E-08		2.51574E-08	1.46877E-08	9.50920E-09
0.00000E+00	0.00000E+00		0.00000E+00	0.00000E+00	0.00000E+00
	8.42946E-05				
6.87117E-01	7.89637E-05		5.83396E-05	3.40606E-05	2.20517E-05
3.61350E-02	4.00940E-06		2.96221E-06	1.72944E-06	1.11968E-06
2.46398E-02	1.32148E-06		9.76333E-07	5.70016E-07	3.69042E-07
	6.79066E-02	8.84E-02	7.32571E-02	7.95559E-02	8.26714E-02
1.89513E+02	6.71528E-02	8.74E-02	7.24440E-02	7.86728E-02	8.17537E-02
2.30507E+00	7.53763E-04	9.81E-04	8.13154E-04	8.83070E-04	9.17652E-04
	1.10574E-07				
3.69587E-05	2.18936E-08	1.59E-08	2.03282E-08	1.84853E-08	1.75738E-08
1.64598E-04	8.86803E-08	6.40E-08	8.22342E-08	7.46457E-08	7.08923E-08
	4.71552E-05				
4.00777E-01	4.70406E-05		3.47544E-05	2.02908E-05	1.31367E-05
1.62243E-04	2.02126E-08		1.49334E-08	8.71859E-09	5.64463E-09
9.04145E-04	9.43019E-08		6.96717E-08	4.06767E-08	2.63351E-08
0.00000E+00	0.00000E+00		0.00000E+00	0.00000E+00	0.00000E+00
0.00000E+00	0.00000E+00		0.00000E+00	0.00000E+00	0.00000E+00
1.84306E-03	5.87968E-06		4.34400E-06	2.53617E-06	1.64198E-06
6.89893E-02	1.58400E-05		1.17028E-05	6.83251E-06	4.42353E-06

Table A-4. Dimensions and volumes of control rod

WCR		O.R. (cm)	o.d. (mm)	i.d. (mm)	thick (mm)	Area (mm²)	Fraction of Homogenized Volume			66		annvol	totlvol	totalwidth
							RZ	3D						
Reflector	Graphite	3.722415	74.44829	45	14.72415	2763	0.007439445	0.634644571	0.6346446	928.5		8.79387	13.85637	3.722415
Channel	Air	2.25	45	22	11.5	1210	0.003259141	0.278030971	0.278031	895.5	862.5	3.8525	5.0625	2.25
WCR Outer Tube	Stl 4541	1.1	22	14	4	226	0.000609106	0.051961661	0.0519617			0.72	1.21	1.10
Gap	Air	0.7	14	13.5	0.25	11	2.90806E-05	0.002480808	0.0024808			0.034375	0.49	0.70
WCR inner Tube	Stl 4301	0.675	13.5	9.5	2	72	0.000194576	0.016598864	0.0165989			0.23	0.455625	0.675
Inside the tube*	Air	0.475	9.5	0	4.75	71	0.000190874	0.016283125	0.0162831			0.225625	0.225625	0.475
ACR		Distance from Core Center			890									
Reflector	Graphite	3.722415	74.44829	55	9.724145	1977	0.005324493	0.454222138						
Channel*	Air	2.75	55	44	5.5	855	0.002303183	0.19648003						
ACR Tube	Al	2.2	44	40	2	264	0.000710624	0.060621938						
Gap (Eq)	Air	2	40	12.220925	13.88954	1139	0.003068053	0.261729624						
ACR Bar (full)	Cu	0.611046	12.22092	0	6.110462	117	0.00031587	0.026946271	Full Cu Thickness					
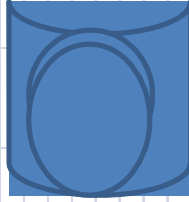
Table A-5. Dimensions and volumes of control rod

WCR — Annulus	3 C	4 O	32 H	26 N	23 Fe56	31 Cr52	22 B10eq	25 B11	5 Si28	27 Si29	28 Si30	24 Al27	29 Cu63	30 Cu65
6	8.84E-02						1.59E-08	6.40E-08						
5		1.00E-05	5.80E-07	4.00E-05		0.1550115			0.009223	0.000467	0.00031			
4					0.624155		0.000344271							
3		1.00E-05	5.80E-07	4.00E-05		0.1550115			0.009223	0.000467	0.00031			
2					0.625347		0.00034276							
1		1.00E-05	5.80E-07	4.00E-05										
RZ Curtain	8.80E-02	3.48E-08	2.02E-09	1.39E-07	5.02E-04	1.25E-04	2.92E-07	6.37E-08	3.19E-05	1.61E-06	1.07E-06	0	0	0
3D Node	5.61E-02	2.97E-06	1.72E-07	1.19E-05	4.28E-02	1.06E-02	2.36E-05	4.06E-08	2.72E-03	1.38E-04	9.13E-05	0	0	0

ACR — Annulus	C	O	H	N	Fe56	Cr52	B10eq	B11	Si28	Si29	Si30	Al27	Cu63	Cu65
5	8.84E-02						1.59E-08	6.40E-08						
4		1.00E-05	5.80E-07	4.00E-05										
3						0						0.056514		
2		1.00E-05	5.80E-07	4.00E-05										
1													0.058734	0.026179
RZ Curtain	8.78E-02	5.37E-08	3.12E-09	2.15E-07	0.00E+00	0.00E+00	1.58E-08	6.36E-08	0.00E+00	0.00E+00	0.00E+00	4.02E-05	1.86E-05	8.27E-06
3D Node	4.01E-02	4.58E-06	2.66E-07	1.83E-05	0.00E+00	0.00E+00	7.22E-09	2.91E-09	0.00E+00	0.00E+00	0.00E+00	3.43E-03	1.58E-03	7.05E-04

BCR (RZ only) — Annulus	C	O	H	N	Fe56	Cr52	B10eq	B11	Si28	Si29	Si30	Al27	Cu63	Cu65
6	8.84E-02	0.00E+00					1.59E-08	6.40E-08						
5		1.00E-05	5.80E-07	4.00E-05	0.00E+00				9.22E-03	4.67E-04	3.10E-04			
4					6.24E-01	1.55E-01	3.44E-04							
3		1.00E-05	5.80E-07	4.00E-05	0.00E+00				9.22E-03	4.67E-04	3.10E-04			
2					6.25E-01	1.55E-01	3.43E-04							
1		1.00E-05	5.80E-07	4.00E-05	0.00E+00		0.00E+00							
RZ Curtain	8.84E-02	1.04E-09	6.02E-11	4.15E-09	5.88E-06	1.46E-06	1.91E-08	6.40E-08	3.73E-07	1.89E-08	1.26E-08	4.71E-07	1.86E-05	8.27E-06
No 3D Node	* Micros from ACR model													

NCR	C	O	H	N	Fe56	Cr52	B10eq	B11	Si28	Si29	Si30	Al27	Cu63	Cu65
3D node below WCR	5.61E-02	3.65E-06	2.12E-07	1.46E-05			1.01E-08	4.06E-08						
3D node above ACR	4.01E-02	5.46E-06	3.17E-07	2.18E-05			7.22E-09	2.91E-09						

39

A-2. Sample PEBBED Input (LP4_16gRZBCR_het.inp)

```
00001  LEU-PRO Heterogeneous Core 4.2 BCR Wedge  16 groups  6/10
= This is used to generate micro xs for the ACR for use in the RZ model.
=     ptyp ndim geo sdim NR NQ NZ
00002  1   2   1 2 62   1 112
=      R   Q    Z   (from Z-R)
00003  1 0 1 1 0 0   1
00005  1.E-4 1.0-6 1.0E-4 1.0E-4 0.002 0.1 1.0E-4
=
00004  5 2 100 1000 20 10 10 5
00006  2 0 0
=00004   1 1 2 1000 20 10 10 5
=00006   1 1 0
=
00007  16 6 1 3
=      CHI and EMAX
00081  1.0 0.0 0.0 0.0 0.0 0.0 0.0 0.0
00082  0.0 0.0 0.0 0.0 0.0 0.0 0.0 0.0
00091  2.000E7 3.68E6 8.21E5 1.83E5 3.18E4 7101. 1234. 354.
00092  78.89 13.71 2.3824 1.9 1.5 0.89 0.42 0.12
00010  32 45 -149 1
19000  0.005
20000  cmbpeb16gvall
00011  1.43 1.0129 0.5
19000  -1.
00012  3
00013  1 0
00015  4 2 0 0 0 0
=
00050  1.0 1.0E-8 1.0E-8
00060  5. 1.
= Uniform velocity profile
00070  0.0 0.0
=
=   radial mesh
= (zone boundaries
=00101 no inner reflector
= core (62.5cm)
00102  5  -3 9.5 -3 10.3 -8 23.7 -3 9.4 -4 9.6
=   graphite reflector and CR curtain
00103  4 8 23.75 3 6.6 10 35.15 10 35.1
=   concrete containment
00104  1 10 50.0
=
=   azimuthal mesh
=00201   5 1 35. 1 35. 1 7.89 1 4.22 1 7.89
=00202   4 1 22.5 1 22.5 1 22.5 1 22.5
=00203   5 1 13. 1 7.39 1 4.22 1 8.39  1 19.
=00204   5 1 38. 1 22.5 1 22.5 1 22.5 1 22.5
00201  1 1 360.
=
=   axial mesh
=
=       top reflector
00301  4 5 15.0  9 27.4 7 26.0 4 10.0
= Al hanger, and void
00302  2 3 15.9 4 21.1
=       core (152cm)
00303  4 -5 15. -8 21.9 -9 27.0 -9 26.7
00304  4 -7 20.9 -7 20.5 -4 12. -4 8.0
=       bottom reflector and concrete
00305  5 7 19. 4 12.0 6 17. 6 18.0 4 12.0
=
=
= Pebble Specs
00700  5 1
00701  10. 0.0 0. 0. 0.
00702  LEUPRO GRAFIT WEDGE1 WEDGE2 WEDGE3
```

```
00703  1.0 0.0 1.0 1.0 1.0
00704  1 30 6 7 8
00705  0 0 0 0 0
00708  0.5 0.5 0. 0. 0.
00711  1 1 1 1 1
00712  9394 0 9394 9394 9394
00713  0.0251 0.0251 0.0251 0.0251 0.0251
00714  2.35  0.0 2.35 2.35 2.35
00715  3.78   3.0 8.3098 9.9983 11.5891              !Eff radii due to mod pebs & wedges
00716  0.2897 0.2897 0.2897 0.2897 0.2897
01600  0.0255
01601  5 61  0.03207  62 0.02890  63 0.02579  64 0.02787  65 0.02005          !0.0255 mean
01602  5 71  0.03207  72 0.02890  73 0.02579  74 0.02787  75 0.02005
01603  5 81  0.03207  82 0.02890  83 0.02579  84 0.02787  85 0.02005
01604  5 91  0.03207  92 0.02890  93 0.02579  94 0.02787  95 0.02005
01605  5 101 0.03207 102 0.02890 103 0.02579 104 0.02787 105 0.02005
01606  5 111 0.03207 112 0.02890 113 0.02579 114 0.02787 115 0.02005
01607  5 121 0.03207 122 0.02890 123 0.02579 124 0.02787 125 0.02005
01608  5 131 0.03207 132 0.02890 133 0.02579 134 0.02787 135 0.02005
00720  5 1 3 4
= layer nuclide IDs
=     C  Si O  B10 B11
00721  3 5 4 22 25
= adsorbed kernel moderator IDs (up to 3 which must be among the composition list)
=      0
00722  4
= adsorbed kernel absorber IDs (up to 3 which must be among the composition list)
=     U25 U28 U24
00723  1 2 21
=  Coolant Nuclide ids and densities (He can be computed)
=      N  O  C  H
00724  26 4 3 32
00725  5.8E-7 1.0E-5 1.0E-8 5.8E-7
=Layer thicknesses
00731  9.15E-03 3.99E-03 3.53E-03 4.0E-03 0.0656      ! LEUPRO
00732  9.15E-03 3.99E-03 3.53E-03 4.0E-03 0.0656      ! MODPEB
00733  9.15E-03 3.99E-03 3.53E-03 4.0E-03 0.0656      ! WEDGE1
00734  9.15E-03 3.99E-03 3.53E-03 4.0E-03 0.0656      ! WEDGE2
00735  9.15E-03 3.99E-03 3.53E-03 4.0E-03 0.0656      ! WEDGE3
= kernel densities
=     C Si O B-10 He-4
00741  0. 0. 4.86157E-02 0. 0. !Spec
00742  0. 0. 4.86157E-02 0. 0.
00743  0. 0. 4.86157E-02 0. 0.
00744  0. 0. 4.86157E-02 0. 0.
00745  0. 0. 4.86157E-02 0. 0.
= shell densities
=        C  H  O   B-10 B-11
00746  8.64535E-02 0. 0. 7.43588E-09 3.01191E-08   !LEUPRO   SPEC
00747  8.44677E-02 1.13E-05 0. 3.19200E-08 1.29292E-07    !MODPEB
00748  8.64535E-02 0. 0. 7.43588E-09 3.01191E-08    !WEDJ3
00749  8.64535E-02 0. 0. 7.43588E-09 3.01191E-08    !WEDJ4
00750  8.64535E-02 0. 0. 7.43588E-09 3.01191E-08    !WEDJ5
= coating densities C, Si, O
=Layer 1 Buffer
=        C, Si, O    B-10, He-4
00751  5.51511E-02 0. 0. 5.46193E-09 2.21236E-08    ! LEUPRO SPEC
00752  5.51511E-02 0. 0. 5.46193E-09 2.21236E-08
00753  5.51511E-02 0. 0. 5.46193E-09 2.21236E-08
00754  5.51511E-02 0. 0. 5.46193E-09 2.21236E-08
00755  5.51511E-02 0. 0. 5.46193E-09 2.21236E-08
=Layer 2 IPyC
00761  9.52609E-02 0. 0. 9.43423E-09 3.82134E-08    ! LEUPRO SPEC
00762  9.52609E-02 0. 0. 9.43423E-09 3.82134E-08
00763  9.52609E-02 0. 0. 9.43423E-09 3.82134E-08
00764  9.52609E-02 0. 0. 9.43423E-09 3.82134E-08
00765  9.52609E-02 0. 0. 9.43423E-09 3.82134E-08
=Layer 3 SiC
00771  4.80603E-02 4.80603E-02 0. 4.75968E-09 1.92791E-08  !LEUPRO SPEC
00772  4.80603E-02 4.80603E-02 0. 4.75968E-09 1.92791E-08
00773  4.80603E-02 4.80603E-02 0. 4.75968E-09 1.92791E-08
```

```
00774  4.80603E-02 4.80603E-02 0. 4.75968E-09 1.92791E-08
00775  4.80603E-02 4.80603E-02 0. 4.75968E-09 1.92791E-08
=Layer 4 OPyC
=00781  9.476E-02 0. 0. 0. 0. !SPREADSHEET
00781  9.47595E-02 0. 0. 9.38457E-09 3.80122E-08  !SPEC
00782  9.47595E-02 0. 0. 9.38457E-09 3.80122E-08
00783  9.47595E-02 0. 0. 9.38457E-09 3.80122E-08
00784  9.47595E-02 0. 0. 9.38457E-09 3.80122E-08
00785  9.47595E-02 0. 0. 9.38457E-09 3.80122E-08
=Layer 5 matrix
00791  8.64535E-02 0. 0. 7.43588E-09 3.01191-08    !LEUPRO  SPEC
00792  8.64535E-02 0. 0. 7.43588E-09 3.01191-08    !MODPEB
00793  8.64535E-02 0. 0. 7.43588E-09 3.01191-08    !WEDJR3
00794  8.64535E-02 0. 0. 7.43588E-09 3.01191-08    !WEDJR4
00795  8.64535E-02 0. 0. 7.43588E-09 3.01191-08    !WEDJR5
=
=
=  Initial Zone Temperatures (K)
= Hall Temp = 19.2C
01500  292.35
= Reflector Temps(2.47m,2.15m,2.63m)
=01501  3  R1 292.85 R1 292.75 R1 292.65
=
=  Composition Map (ACR wedge - 3D only)
=02101  32  9 26 27 28 33 33 33 33 29
=02102  32  9 26 27 28  9 34  9  9 29
=02103  32  9 26 27 28  9 34  9  9 29
=02104  32 24 25 25 28  9 35  9  9 29
=02105  42 42 27 43 43 44 36  9  9 29
=02106  42 42 42 42 22  9 37  9  9 29
=02107   1  2  3  4  5  9 38  9  9 29
=02108   1  2  3  4  5  9 39  9  9 29
=02109   1  2  3  4  5  9 40  9  9 29
=02110   1  2  3  4  5  9 17  9  9 29
=02111   1  2  3  4  5  9 18  9  9 29
=02112   1  2  3  4  5  9 19  9  9 29
=02113   1  2  3  4  5  9 20  9  9 29
=02114   1  2  6  7  8  9 21  9  9 29
=02115   9  9 31 32  9  9 22  9  9 29
=02116   9  9 31 32  9  9 23  9  9 29
=02117   9  9 31 32  9  9 34  9  9 29
=02118   9  9 31 32  9  9 34  9  9 29
=02119   9  9 31 32  9  9 34  9  9 29
=
=
=  Composition Map (WCR wedge - 3D only)
=02101  32  9 26 27 28 33 45 33 33 29
=02102  32  9 26 27 28  9 10  9  9 29
=02103  32  9 26 27 28  9 10  9  9 29
=02104  32 24 25 25 28  9 10  9  9 29
=02105  42 42 27 43 43 44 10  9  9 29
=02106  42 42 42 42 22  9 10  9  9 29
=02107   1  2  3  4  5  9 10  9  9 29
=02108   1  2  3  4  5  9 10  9  9 29
=02109   1  2  3  4  5  9 10  9  9 29
=02110   1  2  3  4  5  9 34  9  9 29
=02111   1  2  3  4  5  9 34  9  9 29
=02112   1  2  3  4  5  9 34  9  9 29
=02113   1  2  3  4  5  9 34  9  9 29
=02114   1  2  6  7  8  9 34  9  9 29
=02115   9  9 31 32  9  9 34  9  9 29
=02116   9  9 31 32  9  9  9  9  9 29
=02117   9  9 31 32  9  9  9  9  9 29
=02118   9  9 31 32  9  9  9  9  9 29
=02119   9  9 31 32  9  9  9  9  9 29
=
=  Composition Map (NCR wedge - 3D only)
=02101  32  9 26 27 28 33 33 33 33 29
=02102  32  9 26 27 28  9  9  9  9 29
=02103  32  9 26 27 28  9  9  9  9 29
=02104  32 24 25 25 28  9  9  9  9 29
```

```
=02105   42 42 27 43 43 44  9  9  9 29
=02106   42 42 42 42 22  9  9  9  9 29
=02107    1  2  3  4  5  9  9  9  9 29
=02108    1  2  3  4  5  9  9  9  9 29
=02109    1  2  3  4  5  9  9  9  9 29
=02110    1  2  3  4  5  9  9  9  9 29
=02111    1  2  3  4  5  9  9  9  9 29
=02112    1  2  3  4  5  9  9  9  9 29
=02113    1  2  3  4  5  9  9  9  9 29
=02114    1  2  6  7  8  9  9  9  9 29
=02115    9  9 31 32  9  9  9  9  9 29
=02116    9  9 31 32  9  9  9  9  9 29
=02117    9  9 31 32  9  9  9  9  9 29
=02118    9  9 31 32  9  9  9  9  9 29
=02119    9  9 31 32  9  9  9  9  9 29
=
=  Composition Map (BCR wedge - RZ only)
02101   32  9 26 27 28 33 45 33 33 29
02102   32  9 26 27 28  9 10  9  9 29
02103   32  9 26 27 28  9 10  9  9 29
02104   32 24 25 25 28  9 11  9  9 29
02105   42 42 27 43 43 44 12  9  9 29
02106   42 42 42 42 22  9 13  9  9 29
02107    1  2  3  4  5  9 14  9  9 29
02108    1  2  3  4  5  9 15  9  9 29
02109    1  2  3  4  5  9 16  9  9 29
02110    1  2  3  4  5  9 17  9  9 29
02111    1  2  3  4  5  9 18  9  9 29
02112    1  2  3  4  5  9 19  9  9 29
02113    1  2  3  4  5  9 20  9  9 29
02114    1  2  6  7  8  9 21  9  9 29
02115    9  9 31 32  9  9 22  9  9 29
02116    9  9 31 32  9  9 23  9  9 29
02117    9  9 31 32  9  9  9  9  9 29
02118    9  9 31 32  9  9  9  9  9 29
02119    9  9 31 32  9  9  9  9  9 29
=
=  Nuclides not in set 1
22100   U-234
22110   1.01  0.0 0.0 0.0 0.0 0.0
22120   9225 0 0
=
22200   B-10
22210   1.01  0.0 0.0 0.0 0.0 0.0
22220   525 0 0
=
22300   Fe-56
22310   56.00  0.0 0.0 0.0 0.0 0.0
22320   2631 1 0
=
22400   Al-27
22410   26.98 0.0 0.0 0.0 0.0 0.0
22420   1325 1 0
=
22500   B-11
22510   11.01  0.0 0.0 0.0 0.0 0.0
22520   528 0 0
=
22600   N-14
22610   14.00  0.0 0.0 0.0 0.0 0.0
22620   725 0 0
=
22700   Si-29
22710   28.98  0.0 0.0 0.0 0.0 0.0
22720   1428 1 0
=
22800   Si-30
22810   29.97  0.0 0.0 0.0 0.0 0.0
22820   1431 1 0
=
22900   Cu-63
```

```
22910   63.00  0.0 0.0 0.0 0.0 0.0
22920   2925 1 0
=
23000   Cu-65
23010   65.00  0.0 0.0 0.0 0.0 0.0
23020   2931 1 0
=
23100   Cr-52
23110   52.00  0.0 0.0 0.0 0.0 0.0
23120   2431 1 0
=
23200   H-1
23210   1.008  0.0 0.0 0.0 0.0 0.0
23220   125 1 0
=
=
= Compositions 1-5 are identical if a single packing fraction is used.
30100   CORER1
30101   13
=     GEO #REG #NUC
30102   3 3 5
=       C U25 U28 O Si28 U26 U24 B10
30111   3 1 2 4 5 16 21 22
=       H B11 N14 Si29 Si30
30112   32 25 26 27 28
= new number densities that reflect 50/50 mix with mod pebbles (eff pebble with large shell)
=pf = 0.5853 (exp core mean)
30121   .06713 6.6322-6 3.2523-5 4.612-5 7.658-5 3.302-8 5.380-8 2.171-8
30122   5.891-6 8.795E-08 1.659E-05 3.888E-06 1.282E-06
=pf = 0.604 (R1 from PEBDAN)
30121   .06791 6.8389-6 3.3537-5 4.716-5 7.896-5 3.405-8 5.548-8 2.189-8
30122   5.890-6 8.868E-08 1.659E-05 4.0094E-06 1.3215E-06
=======================================================================
=
30200   CORER2
30201   13
=     GEO #REG #NUC
30202   3 3 5
=       C U25 U28 O Si28 U26 U24 B10
30211   3 1 2 4 5 16 21 22
=       H B11 N14 Si29 Si30
30212   32 25 26 27 28
= new number densities that reflect 50/50 mix with mod pebbles (eff pebble with large shell)
=pf = 0.5853 (exp core mean)
30221   .06713 6.6322-6 3.2523-5 4.612-5 7.658-5 3.302-8 5.380-8 2.171-8
30222   5.891-6 8.795E-08 1.659E-05 3.888E-06 1.282E-06
=pf = 0.599 (R2 from PEBDAN)
30221   .06770 6.7849-6 3.3272-5 4.688-5 7.834-5 5.504-8 5.504-8 2.185-8
30222   5.891-6 8.849E-08 1.659E-05 3.978E-06 1.311E-06
=
30300   CORER3
30301   13
=     GEO #REG #NUC
30302   3 3 5
=       C U25 U28 O Si28 U26 U24 B10
30311   3 1 2 4 5 16 21 22
=       H B11 N14 Si29 Si30
30312   32 25 26 27 28
= new number densities that reflect 50/50 mix with mod pebbles (eff pebble with large shell)
=pf = 0.5853 (exp core mean)
30321   .06713 6.6322-6 3.2523-5 4.612-5 7.658-5 3.302-8 5.380-8 2.171-8
30322   5.891-6 8.795E-08 1.659E-05 3.888E-06 1.282E-06
=pf = 0.604 (R3 from PEBDAN)
30321   .06791 6.8389-6 3.3537-5 4.716-5 7.896-5 3.405-8 5.548-8 2.189-8
30322   5.890-6 8.868E-08 1.659E-05 4.0094E-06 1.3215E-06
=
30400   CORER4
30401   13
=     GEO #REG #NUC
30402   3 3 5
=       C U25 U28 O Si28 U26 U24 B10
```

```
30411   3 1 2 4 5 16 21 22
=       H B11 N14 Si29 Si30
30412   32 25 26 27 28
= new number densities that reflect 50/50 mix with mod pebbles (eff pebble with large shell)
=pf = 0.5853 (exp core mean)
30421   .06713 6.6322-6 3.2523-5 4.612-5 7.658-5 3.302-8 5.380-8 2.171-8
30422   5.891-6 8.795E-08 1.659E-05 3.888E-06 1.282E-06
=pf = 0.6154 (R4 from PEBDAN)
30421   .06834 6.9542-6 3.4102-5 4.773-5 8.029-5 3.462-8 5.641-8 2.199-8
30422   1.659-5 8.909E-08 1.659E-05 4.077E-06 1.344E-06
=
30500   CORER5
30501   13
=       GEO #REG #NUC
30502   3 3 5
=       C U25 U28 O Si28 U26 U24 B10
30511   3 1 2 4 5 16 21 22
=       H B11 N14 Si29 Si30
30512   32 25 26 27 28
= new number densities that reflect 50/50 mix with mod pebbles (eff pebble with large shell)
=pf = 0.5853 (exp core mean)
30521   .06713 6.6322-6 3.2523-5 4.612-5 7.658-5 3.302-8 5.380-8 2.171-8
30522   5.891-6 8.795E-08 1.659E-05 3.888E-06 1.282E-06
=pf = 0.5433 (R5 from PEBDAN)
30521   .06535 6.1571-6 3.0193-5 4.373-5 7.109-5 3.066-8 4.995-8 2.130-8
30522   5.891-6 8.628E-08 1.6588E-05 1.711E-06 1.190E-06
=
30600   WEJR3
30601   13
=       GEO #REG #NUC
30602   3 3 5
=       C U25 U28 O Si28 U26 U24 B10
30611   3 1 2 4 5 16 21 22
=       H B11 N14 Si29 Si30
30612   32 25 26 27 28
30621   .07311 4.5490-6 2.2307-5 3.223-5 5.252-5 2.265-8 3.690-8 1.989-8
30622   4.352-6 8.046E-08 1.226E-05 2.667E-06 8.790-7
=
30700   WEJR4
30701   13
=       GEO #REG #NUC
30702   3 3 5
=       C U25 U28 O Si28 U26 U24 B10
30711   3 1 2 4 5 16 21 22
=       H B11 N14 Si29 Si30
30712   32 25 26 27 28
30721   .07845 2.656-6 1.302-5 1.882-5 3.066-5 1.322-8 2.154-8 1.823-8
30722   2.541-6 7.361-08 7.155-6 1.557-6 5.132-7
=
30800   WEJR5
30801   13
=       GEO #REG #NUC
30802   3 3 5
=       C U25 U28 O Si28 U26 U24 B10
30811   3 1 2 4 5 16 21 22
=       H B11 N14 Si29 Si30
30812   32 25 26 27 28
30821   .08196 1.719-6 8.432-6 1.218-5 1.985-5 8.561-9 1.395-8 1.741-8
30822   1.645-6 7.022-08 4.632-6 1.008-6 3.225-7
=
30900   REF-100
30901   3
30902   0 0 0
30911   3 22 25
30921   8.83923E-02 1.590E-08 6.400E-08
=
31000   WCRinCore
31001   14
31002   2 6 7
=       C O H N Fe56 Cr52 B10Eq B11 Si28 Si29 Si30 Al Cu63 Cu65
31011   3 4 32 26 23 31 22 25
```

```
31012    5 27 28 24 29 30
31021    5.61E-2 2.97E-6 1.72E-7 1.19E-5 4.28E-2 1.06E-2 2.36E-5 4.06E-8
31022    2.72E-3 1.38E-4 9.13E-5 0. 0. 0.
=    Annuli dimensions and mesh
=        Air  SSTL  Air    SSTL  Air  C
31030    0.475 0.20  0.025  0.40 1.15 1.472  5.
31031    2 1 2 1 2 5
=        Layer nuclides
=        C N Fe56 B10eq Al27 Cu63 Cu65
31040    3 26 23 22 24 29 30
31041    0. 4.0E-5 0. 0. 0. 0. 0. 0.
31042    0. 0. 0.625347 3.4276E-4 0. 0. 0. 0.
31043    0. 4.0E-5 0. 0. 0. 0. 0. 0.
31044    0. 0. 0.624155 3.4427E-4 0. 0. 0. 0.
31045    0. 4.0E-5 0. 0. 0. 0. 0. 0.
31046    8.84E-2 0. 0.0 1.59E-8 0. 0. 0.
=
31100    BCR-Z4  (RZ only)
31101    14
=        C O H N Fe56 Cr52 B10Eq B11 Si28 Si29 Si30 Al Cu63 Cu65
31102    2 -6 7
31111    3 4 32 26 23 31 22 25
31112    5 27 28 24 29 30
31121    8.84E-2 1.04-9 6.02-11 4.15-9 5.88E-6 1.46E-6 1.91E-8 6.40E-8
31122    3.73E-7 1.89E-8 1.26E-8 4.71E-7 1.8149E-5 8.0893E-6
=    Annuli dimensions and mesh
=        Air  SSTL  Air    SSTL  Air  C
31130    0.475 0.20  0.025  0.40 1.15 1.4724  5.
31131    2 1 2 1 2 5
=        Layer nuclides
=        C N Fe56 B10eq Al27 Cu63 Cu65
31140    3 26 23 22 24 29 30
31141    0. 4.0E-5 0. 0. 0. 0. 0. 0.
31142    0. 0. 0.625347 3.3443E-4 0. 0. 0. 0.
31143    0. 4.0E-5 0. 0. 0. 0. 0. 0.
31144    0. 0. 0.624155 3.3443E-4 0. 0. 0. 0.
31145    0. 4.0E-5 0. 0. 0. 0. 0. 0.
31146    8.84E-2 0. 0.0 1.59E-8 0. 0. 0.
=
31200    BCR-Z5
31201    14
=        C O H N Fe56 Cr52 B10Eq B11 Si28 Si29 Si30 Al Cu63 Cu65
31202    2 -6 7
31211    3 4 32 26 23 31 22 25
31212    5 27 28 24 29 30
31221    8.84E-2 1.04-9 6.02-11 4.15-9 5.88E-6 1.46E-6 1.91E-8 6.40E-8
31222    3.73E-7 1.89E-8 1.26E-8 4.71E-7 1.7104E-5 7.6237-6
=    Annuli dimensions and mesh
=        Air  SSTL  Air    SSTL  Air  C
31230    0.475 0.20  0.025  0.40 1.15 1.4724  5.
31231    2 1 2 1 2 5
=        Layer nuclides
=        C N Fe56 B10eq Al27 Cu63 Cu65
31240    3 26 23 22 24 29 30
31241    0. 4.0E-5 0. 0. 0. 0. 0. 0.
31242    0. 0. 0.625347 3.3443E-4 0. 0. 0. 0.
31243    0. 4.0E-5 0. 0. 0. 0. 0. 0.
31244    0. 0. 0.624155 3.3443E-4 0. 0. 0. 0.
31245    0. 4.0E-5 0. 0. 0. 0. 0. 0.
31246    8.84E-2 0. 0.0 1.59E-8 0. 0. 0.
=
31300    BCR-Z6
31301    14
=        C O H N Fe56 Cr52 B10Eq B11 Si28 Si29 Si30 Al Cu63 Cu65
31302    2 -6 7
31311    3 4 32 26 23 31 22 25
31312    5 27 28 24 29 30
31321    8.84E-2 1.04-9 6.02-11 4.15-9 5.88E-6 1.46E-6 1.91E-8 6.40E-8
31322    3.73E-7 1.89E-8 1.26E-8 4.71E-7 1.5612E-5 6.9586E-6
=    Annuli dimensions and mesh
=        Air  SSTL  Air    SSTL  Air  C
```

```
31330    0.475 0.20  0.025   0.40 1.15 1.4724  5.
31331    2 1 2 1 2 5
=      Layer nuclides
=     C N Fe56 B10eq Al27 Cu63 Cu65
31340    3 26 23 22 24 29 30
31341   0. 4.0E-5 0. 0. 0. 0. 0. 0.
31342   0. 0. 0.625347 3.3443E-4 0. 0. 0. 0.
31343   0. 4.0E-5 0. 0. 0. 0. 0. 0.
31344   0. 0. 0.624155 3.3443E-4 0. 0. 0. 0.
31345   0. 4.0E-5 0. 0. 0. 0. 0. 0.
31346   8.84E-2 0. 0.0 1.59E-8 0. 0. 0.
=
31400    BCR-Z7
31401    14
=        C O H N Fe56 Cr52 B10Eq B11 Si28 Si29 Si30 Al Cu63 Cu65
31402    2 -6 7
31411    3 4 32 26 23 31 22 25
31412    5 27 28 24 29 30
31421    8.84E-2 1.04-9 6.02-11 4.15-9 5.88E-6 1.46E-6 1.91E-8 6.40E-8
31422    3.73E-7 1.89E-8 1.26E-8 4.71E-7 1.4156E-5 6.3096E-6
=    Annuli dimensions and mesh
=        Air SSTL Air   SSTL  Air  C
31430    0.475 0.20  0.025   0.40 1.15 1.4724  5.
31431    2 1 2 1 2 5
=      Layer nuclides
=     C N Fe56 B10eq Al27 Cu63 Cu65
31440    3 26 23 22 24 29 30
31441   0. 4.0E-5 0. 0. 0. 0. 0. 0.
31442   0. 0. 0.625347 3.3443E-4 0. 0. 0. 0.
31443   0. 4.0E-5 0. 0. 0. 0. 0. 0.
31444   0. 0. 0.624155 3.3443E-4 0. 0. 0. 0.
31445   0. 4.0E-5 0. 0. 0. 0. 0. 0.
31446   8.84E-2 0. 0.0 1.59E-8 0. 0. 0.
=
31500    BCR-Z8
31501    14
=        C O H N Fe56 Cr52 B10Eq B11 Si28 Si29 Si30 Al Cu63 Cu65
31502    2 -6 7
31511    3 4 32 26 23 31 22 25
31512    5 27 28 24 29 30
31521    8.84E-2 1.04-9 6.02-11 4.15-9 5.88E-6 1.46E-6 1.91E-8 6.40E-8
31522    3.73E-7 1.89E-8 1.26E-8 4.71E-7 1.2668E-5 6.6463E-6
=    Annuli dimensions and mesh
=        Air SSTL Air   SSTL  Air  C
31530    0.475 0.20  0.025   0.40 1.15 1.4724  5.
31531    2 1 2 1 2 5
=      Layer nuclides
=     C N Fe56 B10eq Al27 Cu63 Cu65
31540    3 26 23 22 24 29 30
31541   0. 4.0E-5 0. 0. 0. 0. 0. 0.
31542   0. 0. 0.625347 3.3443E-4 0. 0. 0. 0.
31543   0. 4.0E-5 0. 0. 0. 0. 0. 0.
31544   0. 0. 0.624155 3.3443E-4 0. 0. 0. 0.
31545   0. 4.0E-5 0. 0. 0. 0. 0. 0.
31546   8.84E-2 0. 0.0 1.59E-8 0. 0. 0.
=
31600    BCR-Z9
31601    14
=        C O H N Fe56 Cr52 B10Eq B11 Si28 Si29 Si30 Al Cu63 Cu65
31602    2 -6 7
31611    3 4 32 26 23 31 22 25
31612    5 27 28 24 29 30
31621    8.84E-2 1.04-9 6.02-11 4.15-9 5.88E-6 1.46E-6 1.91E-8 6.40E-8
31622    3.73E-7 1.89E-8 1.26E-8 4.71E-7 1.0696E-5 4.76733E-6
=    Annuli dimensions and mesh
=        Air SSTL Air   SSTL  Air  C
31630    0.475 0.20  0.025   0.40 1.15 1.4724  5.
31631    2 1 2 1 2 5
=      Layer nuclides
=     C N Fe56 B10eq Al27 Cu63 Cu65
31640    3 26 23 22 24 29 30
```

```
31641  0. 4.0E-5 0. 0. 0. 0. 0. 0.
31642  0. 0. 0.625347 3.3443E-4 0. 0. 0. 0.
31643  0. 4.0E-5 0. 0. 0. 0. 0. 0.
31644  0. 0. 0.624155 3.3443E-4 0. 0. 0. 0.
31645  0. 4.0E-5 0. 0. 0. 0. 0. 0.
31646  8.84E-2 0. 0.0 1.59E-8 0. 0. 0.
=
31700   ACR-Z10
31701   14
=       C O H N Fe56 Cr52 B10Eq B11 Si28 Si29 Si30 Al Cu63 Cu65
31702   2 5 7
31711   3 4 32 26 23 31 22 25
31712   5 27 28 24 29 30
= RZ
31721   8.78E-2 5.37E-8 3.12E-9 2.15E-7 0. 0. 1.58E-8 6.36E-8
31722   0. 0. 0. 4.02E-5 8.5301E-6 3.802E-6
=3D
=31721   4.01E-2 5.00E-6 2.90E-7 2.00E-5 0. 0. 7.22E-09 2.91E-8
=31722   0. 0. 0. 3.43E-3 7.2768E-4 3.2434E-04
=    Annuli dimensions and mesh
=        Cu Air Al Air  C
31730   0.41433 1.586 0.2 0.55 0.9724 5.0
31731   3 1 2 1 10
=     Layer nuclides
=        C N Fe56 B10eq Al27 Cu63 Cu65
31740   3 26 23 22 24 29 30
31741  0. 0. 0. 0. 0. 0.058734 0.026179
31742  0. 4.0E-5 0. 0. 0. 0. 0.
31743  0. 0. 0. 0. 0.56514 0. 0.
31744  0. 4.0E-5 0. 0. 0. 0. 0.
31745  8.84E-2 0. 0.0 1.59E-8 0. 0. 0.
=
31800   ACR-Z11
31801   14
=       C O H N Fe56 Cr52 B10Eq B11 Si28 Si29 Si30 Al Cu63 Cu65
31802   2 5 7
31811   3 4 32 26 23 31 22 25
31812   5 27 28 24 29 30
=RZ
31821   4.71E-4 5.86E-8 3.40E-9 2.34E-7 0. 0. 1.58E-8 6.36E-8
31822   0. 0. 0. 4.02E-5 6.6103E-6 2.9643E-6
=3D
=31821   4.01E-2 5.03E-6 2.91E-7 2.00E-5 0. 0. 7.22E-09 2.91E-8
=31822   0. 0. 0. 3.43E-3 5.6391E-04 2.5134E-04
=    Annuli dimensions and mesh
=        Cu Air Al Air  C
31830   0.36474 1.635 0.2 0.55 0.9724 5.0
31831   3 1 2 1 10
=     Layer nuclides
=        C N Fe56 B10eq Al27 Cu63 Cu65
31840   3 26 23 22 24 29 30
31841  0. 0. 0. 0. 0. 0.058734 0.026179
31842  0. 4.0E-5 0. 0. 0. 0. 0.
31843  0. 0. 0. 0. 0.56514 0. 0.
31844  0. 4.0E-5 0. 0. 0. 0. 0.
31845  8.84E-2 0. 0.0 1.59E-8 0. 0. 0.
=
31900   ACR-Z12
31901   14
=       C O H N Fe56 Cr52 B10Eq B11 Si28 Si29 Si30 Al Cu63 Cu65
31902   2 5 7
31911   3 4 32 26 23 31 22 25
31912   5 27 28 24 29 30
=RZ
31921   4.71E-4 5.89E-8 3.42E-9 2.36E-7 0. 0. 1.58E-8 6.36E-8
31922   0. 0. 0. 4.02E-5 4.9406E-6 2.2021E-6
=3D
=31921   4.01E-2 5.05E-6 2.93E-7 2.02E-5 0. 0. 7.22E-09 2.91E-8
=31922   0. 0. 0. 3.43E-3 4.2147E-04 1.8786E-04
=    Annuli dimensions and mesh
=        Cu Air Al Air  C
```

```
31930    0.31533 1.685 0.2 0.55 0.9724 5.0
31931    3 1 2 1 10
=    Layer nuclides
=        C N Fe56 B10eq Al27 Cu63 Cu65
31940    3 26 23 22 24 29 30
31941    0. 0. 0. 0. 0. 0.058734 0.026179
31942    0. 4.0E-5 0. 0. 0. 0. 0.
31943    0. 0. 0. 0. 0.56514 0. 0.
31944    0. 4.0E-5 0. 0. 0. 0. 0.
31945    8.84E-2 0. 0.0 1.59E-8 0. 0. 0.
=
32000    ACR-Z13
32001    14
=        C O H N Fe56 Cr52 B10Eq B11 Si28 Si29 Si30 Al Cu63 Cu65
32002    2 5 7
32011    3 4 32 26 23 31 22 25
32012    5 27 28 24 29 30
=RZ
32021    4.71E-4 5.92E-8 3.43E-9 2.37E-7 0. 0. 1.58E-8 6.36E-8
32022    0. 0. 0. 4.02E-5 3.6298E-6 1.6179E-6
=3D
=32021   4.01E-2 5.07E-6 2.94E-7 2.03E-5 0. 0. 7.22E-09 2.91E-8
=32022   0. 0. 0. 3.43E-3 3.0965E-04 1.3802E-4
=    Annuli dimensions and mesh
=        Cu Air Al Air  C
32030    0.270 1.730 0.2 0.55 0.9724 5.0
32031    3 1 2 1 10
=    Layer nuclides
=        C N Fe56 B10eq Al27 Cu63 Cu65
32040    3 26 23 22 24 29 30
32041    0. 0. 0. 0. 0. 0.058734 0.026179
32042    0. 4.0E-5 0. 0. 0. 0. 0.
32043    0. 0. 0. 0. 0.56514 0. 0.
32044    0. 4.0E-5 0. 0. 0. 0. 0.
32045    8.84E-2 0. 0.0 1.59E-8 0. 0. 0.
=
32100    ACR-Z14
32101    14
=        C O H N Fe56 Cr52 B10Eq B11 Si28 Si29 Si30 Al Cu63 Cu65
32102    2 5 7
32111    3 4 32 26 23 31 22 25
32112    5 27 28 24 29 30
=RZ
32121    4.71E-4 5.94E-8 3.45E-9 2.38E-7 0. 0. 1.58E-8 6.36E-8
32122    0. 0. 0. 4.02E-5 2.8232E-6 1.2583E-6
=3D
=32121   4.01E-2 5.08E-6 2.95E-7 2.03E-5 0. 0. 7.22E-09 2.91E-8
=32122   0. 0. 0. 3.43E-3 2.4084E-04 1.0735E-04
=    Annuli dimensions and mesh
=        Cu Air Al Air  C
32130    0.2384 1.7616 0.2 0.55 0.9724 5.0
32131    3 1 2 1 10
=    Layer nuclides
=        C N Fe56 B10eq Al27 Cu63 Cu65
32140    3 26 23 22 24 29 30
32141    0. 0. 0. 0. 0. 0.058734 0.026179
32142    0. 4.0E-5 0. 0. 0. 0. 0.
32143    0. 0. 0. 0. 0.56514 0. 0.
32144    0. 4.0E-5 0. 0. 0. 0. 0.
32145    8.84E-2 0. 0.0 1.59E-8 0. 0. 0.
=
32200    ACR-Z15
32201    14
=        C O H N Fe56 Cr52 B10Eq B11 Si28 Si29 Si30 Al Cu63 Cu65
32202    2 5 7
32211    3 4 32 26 23 31 22 25
32212    5 27 28 24 29 30
=RZ
32221    4.71E-4 5.95E-8 3.45E-9 2.38E-7 0. 0. 1.58E-8 6.36E-8
32222    0. 0. 0. 4.02E-5 1.7342E-6 7.7298E-7
=3D
```

```
=32221    4.01E-2 5.10E-6 2.96E-7 2.04E-5 0. 0. 7.22E-09 2.91E-8
=32222    0. 0. 0. 3.43E-3 1.4794E-04 6.5941E-05
=    Annuli dimensions and mesh
=        Cu Air Al Air  C
32230   0.18682 1.81318 0.2 0.55 0.9724 5.0
32231   3 1 2 1 10
=    Layer nuclides
=       C N Fe56 B10eq Al27 Cu63 Cu65
32240   3 26 23 22 24 29 30
32241  0. 0. 0. 0. 0. 0.058734 0.026179
32242  0. 4.0E-5 0. 0. 0. 0. 0.
32243  0. 0. 0. 0. 0.56514 0. 0.
32244  0. 4.0E-5 0. 0. 0. 0. 0.
32245  8.84E-2 0. 0.0 1.59E-8 0. 0. 0.
=
32300   ACR-Z16
32301   14
=       C O H N Fe56 Cr52 B10Eq B11 Si28 Si29 Si30 Al Cu63 Cu65
32302   2 5 7
32311   3 4 32 26 23 31 22 25
32312   5 27 28 24 29 30
=RZ
32321   4.71E-4 5.97E-8 3.46E-9 2.39E-7 0. 0. 1.58E-8 6.36E-8
32322   0. 0. 0. 4.02E-5 4.8397E-7 2.1571E-7
=3D
=32321   4.01E-2 5.11E-6 2.97E-7 2.05E-5 0. 0. 7.22E-09 2.91E-8
=32322   0. 0. 0. 3.43E-3 4.1287E-05 1.8402E-05
=    Annuli dimensions and mesh
=        Cu Air Al Air  C
32330   0.09869 1.90131 0.2 0.55 0.9724 5.0
32331   3 1 2 1 10
=    Layer nuclides
=       C N Fe56 B10eq Al27 Cu63 Cu65
32340   3 26 23 22 24 29 30
32341  0. 0. 0. 0. 0. 0.058734 0.026179
32342  0. 4.0E-5 0. 0. 0. 0. 0.
32343  0. 0. 0. 0. 0. 0. 0.56514 0. 0.
32344  0. 4.0E-5 0. 0. 0. 0. 0.
32345  8.84E-2 0. 0.0 1.59E-8 0. 0. 0.
=
32400   TopRef_1
32401   7
32402   1 2 7
=        H O N C B10 B11 Al
32411   32 4 26 3 22 25 24
32421   0.0 0.0 0.0 8.471E-02 1.524E-08 6.133E-08 2.511E-03
=      Layers (slab width & # meshes)
=        Al C
32430   0.400 9.6
32431   4 10
=      Layer nuclides
=      H O N C B10 B11 Al
32440   32 4 26 3 22 25 24
32441  0.0 0.0 0.0 0.0 0.0 0.0 0.0602626
32442  0.0 0.0 0.0 8.83923E-02 1.58E-08 6.4E-08 0.0
=
32500   TopRef_2
32501   7
32502   1 2 7
=        H O N C B10 B11 Al
32511   32 4 26 3 22 25 24
========================================================================
32521   1.6E-8 2.758E-7 1.103E-6 8.429E-2 1.516E-8 6.103E-8 1.109E-3
=      Layers (slab width & # meshes)
=        Al C
32530   0.400 9.6
32531   4 10
=      Layer nuclides
=      H O N C B10 B11 Al
32540   32 4 26 3 22 25 24
32541  0.0 0.0 0.0 0.0 0.0 0.0 0.0602626
```

```
32542  0.0 0.0 0.0 8.83923E-02 1.58E-08 6.4E-08 0.0
=
=
32600   TopRef_3
32601   7
32602   1 2 7
=       H O N C B10 B11 Al
32611   32 4 26 3 22 25 24
====================================================================
32621   1.6E-8 2.758E-7 1.103E-6 8.429E-2 1.516E-8 6.103E-8 8.102E-4
=       Layers (slab width & # meshes)
=        Al C
32630   0.700 14.3
32631   4 10
=       Layer nuclides
=       H O N C B10 B11 Al
32640   32 4 26 3 22 25 24
32641  0.0 0.0 0.0 0.0 0.0 0.0 0.0602626
32642  0.0 0.0 0.0 8.83923E-02 1.58E-08 6.4E-08 0.0
=
32700   TopVoidAl1
32701   7
32702   1 2 7
=       H O N C B10 B11 Al
32711   32 4 26 3 22 25 24
====================================================================
32721   5.554E-7 9.576E-6 3.83E-5 0.0 0.0 0.0 2.297E-3
=       Layers (slab width & # meshes)
=        Al Air
32730   0.400 14.6
32731   4 10
=       Layer nuclides
=       H O N C B10 B11 Al
32740   32 4 26 3 22 25 24
32741  0.0 0.0 0.0 0.0 0.0 0.0 0.0602626
32742  5.8E-7 1.0E-5 4.0E-5 0.0 0.0 0.0 0.0
32780   6.25 1.0 29.39
=
32800   TopRef_5
32801   7
32802   1 2 7
=       H O N C B10 B11 Al
32811   32 4 26 3 22 25 24
====================================================================
32821   0.0 0.0 0.0 8.086E-2 1.454E-8 5.855E-8 1.787E-3
=       Layers (slab width & # meshes)
=        Al C
32830   0.760 8.84
32831   4 10
=       Layer nuclides
=       H O N C B10 B11 Al
32840   32 4 26 3 22 25 24
32841  0.0 0.0 0.0 0.0 0.0 0.0 0.0602626
32842  0.0 0.0 0.0 8.83923E-02 1.58E-08 6.4E-08 0.0
=
32900   CONCRETE
32901   9
32902   0 0 0
=       C Si28 Si29 Si30 Al27 Fe56 H1 O16 B10eq
32911   3 5 27 28 24 23 32 4
32912   22
====================================================================
32921   1.153-3 1.533-2 7.762-4 5.152-4 1.739-3 3.260-4 1.374-2 4.591-2
32922   1.262E-6
=
33000   ModPeb
33001   6
=       GEO #REG #NUC
33002   -3 2 6
=       C B10 B11 O H N
33011   3 22 25 4 32 26
```

51

```
33021    4.9439E-2 1.8683E-8 7.5675E-8 2.7409E-0 8.0125E-6 9.6455E-5
=
33100    REF-97.2
33101    3
33102    0 0 0
33111    3 22 25
33121    8.5954E-02 1.5461E-08 6.2235E-08
=
33200    REF-97.7
33201    3
33202    0 0 0
33211    3 22 25
33221    8.6374E-02 1.5537E-08 6.2539E-08
=
33300    RefVoid
33301    4
33302    0 0 0
=        C O H N
33311    3 4 32 26
33321    1.0E-5 1.0E-5 5.80E-07 4.00E-5
=
33400    Empty_CRC
33401    6
33402    0 0 0
=        C O H N B10eq B11
33411    3 4 32 26 22 25
33421    5.61E-2 3.65E-6 2.12E-7 1.46E-5 1.01E-8 4.06E-8
=
33500    ACR-Z4     (3D only)
33501    14
=        C O H N Fe56 Cr52 B10Eq B11 Si28 Si29 Si30 Al Cu63 Cu65
33502    2 5 7
33511    3 4 32 26 23 31 22 25
33512    5 27 28 24 29 30
33521    4.01E-2 4.86E-6 2.82E-7 1.94E-5 0. 0. 7.22E-9 2.91E-8
33522    0. 0. 0. 3.43E-3 1.5483E-3 6.9008E-4
=    Annuli dimensions and mesh
=        Cu Air Al Air  C
33530    0.60437 1.39563 0.2 0.55 0.9724 5.0
33531    3 1 2 1 10
=      Layer nuclides
=      C N Fe56 B10eq Al27 Cu63 Cu65
33540   3 26 23 22 24 29 30
33541   0. 0. 0. 0. 0. 0.058734 0.026179
33542   0. 4.0E-5 0. 0. 0. 0. 0.
33543   0. 0. 0. 0. 0.56514 0. 0.
33544   0. 4.0E-5 0. 0. 0. 0. 0.
33545   8.84E-2 0. 0.0 1.59E-8 0. 0. 0.
=
33600    ACR-05        (3D only)
33601    14
=        C O H N Fe56 Cr52 B10Eq B11 Si28 Si29 Si30 Al Cu63 Cu65
33602    2 5 7
33611    3 4 32 26 23 31 22 25
33612    5 27 28 24 29 30
33621    4.01E-2 4.87E-6 2.83E-7 1.94E-5 0. 0. 7.22E-9 2.91E-8
33622    0. 0. 0. 3.43E-3 1.4592E-3 6.5036E-4
=    Annuli dimensions and mesh
=        Cu Air Al Air  C
33630    0.58672 1.41328 0.2 0.55 0.9724 5.0
33631    3 1 2 1 10
=      Layer nuclides
=      C N Fe56 B10eq Al27 Cu63 Cu65
33640   3 26 23 22 24 29 30
33641   0. 0. 0. 0. 0. 0.058734 0.026179
33642   0. 4.0E-5 0. 0. 0. 0. 0.
33643   0. 0. 0. 0. 0.56514 0. 0.
33644   0. 4.0E-5 0. 0. 0. 0. 0.
33645   8.84E-2 0. 0.0 1.59E-8 0. 0. 0.
=
33700    ACR-06        (3D only)
```

```
33701   14
=       C O H N Fe56 Cr52 B10Eq B11 Si28 Si29 Si30 Al Cu63 Cu65
33702   2 5 7
33711   3 4 32 26 23 31 22 25
33712   5 27 28 24 29 30
33721   4.01E-2 4.89E-6 2.84E-7 1.96E-5 0. 0. 7.22E-9 2.91E-8
33722   0. 0. 0. 3.43E-3 1.3318E-3 5.9362E-4
=    Annuli dimensions and mesh
=        Cu Air Al Air  C
33730   0.56054 1.43946 0.2 0.55 0.9724 5.0
33731   3 1 2 1 10
=      Layer nuclides
=      C N Fe56 B10eq Al27 Cu63 Cu65
33740   3 26 23 22 24 29 30
33741   0. 0. 0. 0. 0. 0.058734 0.026179
33742   0. 4.0E-5 0. 0. 0. 0. 0.
33743   0. 0. 0. 0. 0.56514 0. 0.
33744   0. 4.0E-5 0. 0. 0. 0. 0.
33745   8.84E-2 0. 0.0 1.59E-8 0. 0. 0.
=
33800   ACR-07       (3D only)
33801   14
=       C O H N Fe56 Cr52 B10Eq B11 Si28 Si29 Si30 Al Cu63 Cu65
33802   2 5 7
33811   3 4 32 26 23 31 22 25
33812   5 27 28 24 29 30
33821   4.01E-2 4.92E-6 2.85E-7 1.97E-5 0. 0. 7.22E-9 2.91E-8
33822   0. 0. 0. 3.43E-3 1.2076E-3 5.3826E-4
=    Annuli dimensions and mesh
=        Cu Air Al Air  C
33830   0.53376 1.46624 0.2 0.55 0.9724 5.0
33831   3 1 2 1 10
=      Layer nuclides
=      C N Fe56 B10eq Al27 Cu63 Cu65
33840   3 26 23 22 24 29 30
33841   0. 0. 0. 0. 0. 0.058734 0.026179
33842   0. 4.0E-5 0. 0. 0. 0. 0.
33843   0. 0. 0. 0. 0.56514 0. 0.
33844   0. 4.0E-5 0. 0. 0. 0. 0.
33845   8.84E-2 0. 0.0 1.59E-8 0. 0. 0.
=
33900   ACR-08       (3D only)
33901   14
=       C O H N Fe56 Cr52 B10Eq B11 Si28 Si29 Si30 Al Cu63 Cu65
33902   2 5 7
33911   3 4 32 26 23 31 22 25
33912   5 27 28 24 29 30
33921   4.01E-2 4.94E-6 2.86E-7 1.97E-5 0. 0. 7.22E-9 2.91E-8
33922   0. 0. 0. 3.43E-3 1.0807E-3 4.8168E-4
=    Annuli dimensions and mesh
=        Cu Air Al Air  C
33930   0.50493 1.49507 0.2 0.55 0.9724 5.0
33931   3 1 2 1 10
=      Layer nuclides
=      C N Fe56 B10eq Al27 Cu63 Cu65
33940   3 26 23 22 24 29 30
33941   0. 0. 0. 0. 0. 0.058734 0.026179
33942   0. 4.0E-5 0. 0. 0. 0. 0.
33943   0. 0. 0. 0. 0.56514 0. 0.
33944   0. 4.0E-5 0. 0. 0. 0. 0.
33945   8.84E-2 0. 0.0 1.59E-8 0. 0. 0.
=
34000   ACR-09       (3D only)
34001   14
=       C O H N Fe56 Cr52 B10Eq B11 Si28 Si29 Si30 Al Cu63 Cu65
34002   2 5 7
34011   3 4 32 26 23 31 22 25
34012   5 27 28 24 29 30
34021   4.01E-2 4.97E-6 2.88E-7 1.99E-5 0. 0. 7.22E-9 2.91E-8
34022   0. 0. 0. 3.43E-3 9.1244E-4 4.0669E-4
=    Annuli dimensions and mesh
```

```
=          Cu Air Al Air   C
34030   0.46396 1.53604 0.2 0.55 0.9724 5.0
34031   3 1 2 1 10
=     Layer nuclides
=      C N Fe56 B10eq Al27 Cu63 Cu65
34040   3 26 23 22 24 29 30
34041  0. 0. 0. 0. 0. 0.058734 0.026179
34042  0. 4.0E-5 0. 0. 0. 0. 0.
34043  0. 0. 0. 0. 0.56514 0. 0.
34044  0. 4.0E-5 0. 0. 0. 0. 0.
34045  8.84E-2 0. 0.0 1.59E-8 0. 0. 0.
=
34100    Above_ACR
34101    6
34102    0 0 0
=       C O H N B10eq B11
34111   3 4 32 26 22 25
34121   4.01E-2 5.46E-6 3.17E-7 2.18E-5 7.22E-9 2.91E-8
=
34200    TopVoid
34201    3
34202    0 0 0
=        H O N
34211   32 4 26
34221   5.8E-7 1.0E-5 4.0E-5
34280   6.25 1.0 29.39
=
34300    TopVoidAl2
34301    7
34302    1 3 4
=        H O N C B10 B11 Al
34311   32 4 26 3 22 25 24
==============================================================
34321   5.411E-7 9.329E-6 3.732E-5 0.0 0.0 0.0 4.044E-3
=     Layers (slab width & # meshes)
=         Air Al Air
34330   7.9 1.00 7.0
34331   4 10 4.0
=     Layer nuclides
=      H O N C B10 B11 Al
34340   32 4 26 3 22 25 24
34341  5.8E-7 1.0E-5 4.0E-5 0.0 0.0 0.0 0.0
34342  0.0 0.0 0.0 0.0 0.0 0.0 0.0602626
34343  5.8E-7 1.0E-5 4.0E-5 0.0 0.0 0.0 0.0
34380   6.25 1.0 29.39
=
34400    RefAl
34401    7
34402    1 3 4
=        H O N C B10 B11 Al
34411   32 4 26 3 22 25 24
==============================================================
34421   0.0 0.0 0.0 8.776E-02 1.579E-08 6.354E-08 4.044E-3
=     Layers (slab width & # meshes)
=         Air Al Air
34430   7.9 1.00 7.0
34431   4 10 4
=     Layer nuclides
=      H O N C B10 B11 Al
34440   32 4 26 3 22 25 24
34441  0.0 0.0 0.0 8.839E-02 1.59E-8 6.133E-8 0.0
34442  0.0 0.0 0.0 0.0 0.0 0.0 0.0602626
34443  0.0 0.0 0.0 8.839E-02 1.59E-8 6.133E-8 0.0
=
34500    WCRexCore
34501    14
34502    2 6 7
=        C O H N Fe56 Cr52 B10Eq B11 Si28 Si29 Si30 Al Cu63 Cu65
34511   3 4 32 26 23 31 22 25
34512   5 27 28 24 29 30
34521   1.0E-10 1.0E-5 5.80E-07 4.00E-5 4.28E-2 1.06E-2 2.36E-5 4.06E-8
```

```
34522   2.72E-3 1.38E-4 9.13E-5 0. 0. 0.
=    Annuli dimensions and mesh
=        Air  SSTL  Air    SSTL  Air  C
34530   0.475 0.20  0.025  0.40 1.15 1.472  5.
34531    2 1 2 1 2 5
=      Layer nuclides
=    C N Fe56 B10eq Al27 Cu63 Cu65
34540    3 26 23 22 24 29 30
34541   0. 4.0E-5 0. 0. 0. 0. 0. 0.
34542   0. 0. 0.625347 3.4276E-4 0. 0. 0. 0.
34543   0. 4.0E-5 0. 0. 0. 0. 0. 0.
34544   0. 0. 0.624155 3.4427E-4 0. 0. 0. 0.
34545   0. 4.0E-5 0. 0. 0. 0. 0. 0.
34546   8.84E-2 0. 0.0 1.59E-8 0. 0. 0.
=
=
40002   1
= Pebble and Coolant T/H Data
50000   0 0 0 0
50001   3.0  2.35 0.5853
= Only useful for helium
50002   20.0  385.0  5196.0 0.0975
50003   8. 50. 1.76
=
.
```

55

```
34522   2.72E-3 1.38E-4 9.13E-5 0. 0. 0.
=    Annuli dimensions and mesh
=        Air  SSTL  Air    SSTL  Air  C
34530   0.475 0.20  0.025  0.40 1.15 1.472  5.
34531    2 1 2 1 2 5
=      Layer nuclides
=    C N Fe56 B10eq Al27 Cu63 Cu65
34540    3 26 23 22 24 29 30
34541   0. 4.0E-5 0. 0. 0. 0. 0. 0.
34542   0. 0. 0.625347 3.4276E-4 0. 0. 0. 0.
34543   0. 4.0E-5 0. 0. 0. 0. 0. 0.
34544   0. 0. 0.624155 3.4427E-4 0. 0. 0. 0.
34545   0. 4.0E-5 0. 0. 0. 0. 0. 0.
34546   8.84E-2 0. 0.0 1.59E-8 0. 0. 0.
=
=
40002   1
= Pebble and Coolant T/H Data
50000   0 0 0 0
50001   3.0  2.35 0.5853
= Only useful for helium
50002   20.0  385.0  5196.0 0.0975
50003   8. 50. 1.76
=
.
```